Dyson indices and Hilbert–Schmidt separability functions and probabilities

2007 J. Phys. A: Math. Theor. 40 14279

(http://iopscience.iop.org/1751-8121/40/47/017)

J. Phys. A: Math. Theor. **40** (2007) 14279–14308 doi:10.1088/1751-8113/40/47/017

Dyson indices and Hilbert–Schmidt separability functions and probabilities

Paul B Slater

ISBER, University of California, Santa Barbara, CA 93106, USA

E-mail: slater@kitp.ucsb.edu

Received 21 May 2007, in final form 11 October 2007
Published 6 November 2007
Online at stacks.iop.org/JPhysA/40/14279

Abstract

A confluence of numerical and theoretical results leads us to conjecture that the Hilbert–Schmidt separability *probabilities* of the 15- and 9-dimensional convex sets of complex and real two-qubit states (representable by 4×4 density matrices ρ) are $\frac{8}{33}$ and $\frac{8}{17}$, respectively. Central to our reasoning are the modifications of two ansätze, recently advanced by Slater (2007 *Phys. Rev.* A **75** 032326), involving incomplete beta functions $B_\nu(a, b)$, where $\nu = \frac{\rho_{11}\rho_{44}}{\rho_{22}\rho_{33}}$. We, now, set the separability *function* $\mathcal{S}_{\text{real}}(\nu)$ proportional to $B_\nu\left(\nu, \frac{1}{2}, 2\right) = \frac{2}{3}(3-\nu)\sqrt{\nu}$. Then, in the *complex* case—conforming to a pattern we find, manifesting the Dyson indices ($\beta = 1, 2, 4$) of random matrix theory—we take $\mathcal{S}_{\text{complex}}(\nu)$ proportional to $\mathcal{S}^2_{\text{real}}(\nu)$. We also investigate the real and complex qubit–*qutrit* cases. Now, there are *two* variables, $\nu_1 = \frac{\rho_{11}\rho_{55}}{\rho_{22}\rho_{44}}$, $\nu_2 = \frac{\rho_{22}\rho_{66}}{\rho_{33}\rho_{55}}$, but they appear to remarkably coalesce into the product $\eta = \nu_1\nu_2 = \frac{\rho_{11}\rho_{66}}{\rho_{33}\rho_{44}}$, so that the real and complex separability functions are again *univariate* in nature.

PACS numbers: 03.67.−a, 02.30.Cj, 02.40.Dr, 02.40.Ft
Mathematics Subject Classification: 81P05, 52A38, 15A90, 81P15

(Some figures in this article are in colour only in the electronic version)

1. Introduction

Życzkowski and Sommers have derived—using random matrix theory (in particular, the Laguerre ensemble)—general formulas for the (n^2-1)-dimensional and the $\left(\frac{n(n+1)-2}{2}\right)$-dimensional volumes of the complex and real $n \times n$ density matrices (ρ), respectively, in terms of the Hilbert–Schmidt (HS) metric [1] and [2, section 14.3] (as well as the Bures metric [2, section 14.4] and [3, 4]). Later, Andai [5] examined these and related questions, using a quite different framework. He applied mathematical induction on the leading principal minors of ρ, along with the established formulas for hyperareas of surfaces of n-spheres and beta

integrals. He reproduced—up to normalization factors—the HS real and complex volume formulas in [1] (and, moreover, the $(2n^2 - n - 1)$-dimensional quaternionic volumes). (In addition to the HS and Bures metrics, Andai considered, for the single-qubit case, the broad (infinitely nondenumerable) class—which does include the Bures as its minimal member—of monotone metrics. Unlike Życzkowski and Sommers, he did not obtain formulas for the hyperareas occupied by density matrices of *less* than full rank.)

Despite these considerable theoretical advances, volume (and, hence, probability) formulas have not yet become available for the important subsets of separable ($n \leqslant 6$) and positive-partial-transpose ($n \geqslant 8$) $n \times n$ density matrices (n composite). (Szarek [6] employed methods of *asymptotic* convex geometry to *estimate* the volume of the set of separable mixed quantum states for N qudits, and Aubrun and Szarek [7] for N qubits. It was concluded in these studies that the separable volumes were super-exponentially small in the dimension of the set of states. For large D, the $(D^2 - 1)$-dimensional volume for bipartite systems of positive-partial-transpose states, however, is much larger than the volume of separable states [7, theorem 4].)

To address this fundamental lacuna, at least in the Hilbert–Schmidt context (cf [8]), we developed in [9] a methodology—incorporating the Bloore parameterization of density matrices [10] (section 1.1). Its numerical application led to ansätze, involving (apparently independent) incomplete beta functions, for the 9-dimensional real and 15-dimensional complex separable volumes in the qubit–qubit ($n = 4$) case [9]. Following to that study here, we, first, apply this Bloore framework to various scenarios involving $n \times n$ density matrices ($n = 4, 6, 8, 9$), in which certain of their off-diagonal entries have been *nullified*. This enables us to now obtain *exact* results, of interest in themselves, and possibly suggestive of solutions/approaches to the full (non-nullified) highly computationally challenging problems.

In fact, based on certain (real–complex-quaternionic) patterns emerging in these exact results (section 2.1.4), bearing an obvious relation to the Dyson indices ($\beta = 1, 2, 4$) of random matrix theory [11], we are led to modify the incomplete beta function ansätze for the two full (real and complex) problems advanced in [9]. The 'separability function' in the complex case is now *not* analyzed as if it were independent of that in the real case (which we still take to be an incomplete—but slightly different—beta function), but actually simply proportional to its *square*. These central analyses will be elaborated upon in section 9, (equations (94)–(96)), where it is shown that the modified ansätze do, in fact, accord well (figure 3) with the numerical results of [9].

We begin our extensive series of lower dimensional analyses, by examining a number of two-qubit scenarios (section 2). In them, we are able to compute a number of interesting exact two-qubit scenario-specific HS separability probabilities. (Listing them in increasing order, we have $\{\frac{1}{10}, \frac{1}{3}, \frac{3}{8}, \frac{2}{5}, \frac{135\pi}{1024}, \frac{16}{3\pi^2}, \frac{3\pi}{16}, \frac{5}{8}, \frac{105\pi}{512}, 2 - \frac{435\pi}{1024}, \frac{11}{16}, 1\}$.) For each of the scenarios, we identify a certain univariate separability function $\mathcal{S}_{\text{scenario}}(\nu)$, where $\nu = \frac{\rho_{11}\rho_{44}}{\rho_{22}\rho_{33}}$. The integral over $\nu \in [0, \infty]$ of the product of this function (typically of a *piecewise* nature over [0,1] and $[1, \infty]$) with a scenario-specific (marginal) Jacobian function $\mathcal{J}_{\text{scenario}}(\nu)$ yields the HS *separable* volume $\left(V_{\text{sep}}^{\text{HS}}\right)$. The ratio of $V_{\text{sep}}^{\text{HS}}$ to the HS *total* (entangled and non-entangled) volume $\left(V_{\text{tot}}^{\text{HS}}\right)$ gives us the HS scenario-specific separability *probability*.

The question of the 'relative proportion' of entangled and non-entangled states in a given generic class of composite quantum systems, had apparently first been raised by Życzkowski, Horodecki, Sanpera and Lewenstein (ZHSL) in a much-cited paper [12]. They gave 'three main reasons'—'philosophical', 'practical' and 'physical'—upon which they expanded, for pursuing the topic. The present author, motivated by the ZHSL paper, has investigated this issue in a number of settings, using various (monotone and non-monotone) measures on quantum states, and a variety of numerical and analytical methods [4, 13–19] (cf [20–23]). Though

the problems are challenging (high dimensional) in nature, many of the results obtained in answer to the ZHSL question in these various contexts have been strikingly simple and elegant (and/or conjecturally so).

Specifically here, we further develop the (Bloore-parameterization-based) approach presented in [9]. This was found to be relatively effective in studying the question posed by ZHSL, in the context of two-qubit systems (the smallest possible example exhibiting entanglement), endowed with the (non-monotone [24]) *Hilbert–Schmidt* (HS) measure [1], inducing the flat, *Euclidean* geometry on the space of 4×4 density matrices. This approach [9] exploits two distinct features of a form of density matrix parameterization first discussed by Bloore [10]. These properties allow us to deal with lower dimensional integrations (more amenable to computation) than would otherwise be possible. We further find that the interesting advantages of the Bloore parameterization do, in fact, carry over—in a somewhat modified fashion—to the qubit–qutrit (section 3 and 10.1), qutrit–qutrit (section 4) and qubit–qubit–qubit (sections 5 and 6) domains.

1.1. Bloore (off-diagonal-scaling) parameterization

We, first, consider the nine-dimensional convex set of (two-qubit) 4×4 density matrices with *real* entries, and parameterize them—following Bloore [10] (cf [25, p 235])—as

$$\rho = \begin{pmatrix} \rho_{11} & z_{12}\sqrt{\rho_{11}\rho_{22}} & z_{13}\sqrt{\rho_{11}\rho_{33}} & z_{14}\sqrt{\rho_{11}\rho_{44}} \\ z_{12}\sqrt{\rho_{11}\rho_{22}} & \rho_{22} & z_{23}\sqrt{\rho_{22}\rho_{33}} & z_{24}\sqrt{\rho_{22}\rho_{44}} \\ z_{13}\sqrt{\rho_{11}\rho_{33}} & z_{23}\sqrt{\rho_{22}\rho_{33}} & \rho_{33} & z_{34}\sqrt{\rho_{33}\rho_{44}} \\ z_{14}\sqrt{\rho_{11}\rho_{44}} & z_{24}\sqrt{\rho_{22}\rho_{44}} & z_{34}\sqrt{\rho_{33}\rho_{44}} & \rho_{44} \end{pmatrix}. \tag{1}$$

One, of course, has the standard requirements that $\rho_{ii} \geqslant 0$ and (the unit trace condition) $\Sigma_i \rho_{ii} = 1$. Now, three additional necessary conditions (which can be expressed *without* using the diagonal entries, due to the $\rho_{ii} \geqslant 0$ stipulation) that must be fulfilled for ρ to be a density matrix (with all eigenvalues non-negative) are (1) the non-negativity of the determinant (the principal 4×4 minor),

$$\begin{aligned} \left(z_{34}^2 - 1\right) z_{12}^2 + 2(z_{14}(z_{24} - z_{23}z_{34}) + z_{13}(z_{23} - z_{24}z_{34}))z_{12} - z_{23}^2 - z_{24}^2 - z_{34}^2 \\ + z_{14}^2\left(z_{23}^2 - 1\right) + z_{13}^2\left(z_{24}^2 - 1\right) + 2z_{23}z_{24}z_{34} + 2z_{13}z_{14}(z_{34} - z_{23}z_{24}) + 1 \geqslant 0; \end{aligned} \tag{2}$$

(2): the non-negativity of the leading principal 3×3 minor,

$$-z_{12}^2 + 2z_{13}z_{23}z_{12} - z_{13}^2 - z_{23}^2 + 1 \geqslant 0; \tag{3}$$

and (3): the non-negativity of the principal 2×2 minors (although actually only the $i = j = 1$ case is needed, it is natural to impose them all),

$$1 - z_{ij}^2 \geqslant 0. \tag{4}$$

As noted, the *diagonal* entries of ρ do *not* enter into any of these constraints—which taken together are *sufficient* to guarantee the non-negativity of ρ itself—as they can be shown to contribute only (cancelable) non-negative factors to the determinant and principal minors. This cancelation property is certainly a principal virtue of the Bloore parameterization, allowing one to proceed analytically in lower dimensions than one might initially surmise. (Let us note that, utilizing this parameterization, we have been able to establish a recent conjecture of Månsson, Porta Mana and Björk regarding Bayesian state assignment for three-level quantum systems, and, in fact, verify our own four-level analogue of their conjecture ([26], equation (52)) [27].)

Additionally, implementing the Peres–Horodecki condition [28–30] requiring the non-negativity of the *partial transposition* of ρ, we have the necessary *and* sufficient condition for the *separability* (non-entanglement) of ρ that (4):

$$\begin{aligned}\nu\left(z_{34}^2-1\right)z_{12}^2+2\sqrt{\nu}(\nu z_{13}z_{14}+z_{23}z_{24}-\sqrt{\nu}(z_{14}z_{23}+z_{13}z_{24})z_{34})z_{12}-z_{23}^2-\nu z_{34}^2+\nu\\ +\nu\left(\left(z_{24}^2-1\right)z_{13}^2-2z_{14}z_{23}z_{24}z_{13}-z_{24}^2+z_{14}^2\left(z_{23}^2-\nu\right)\right)\\ +2\sqrt{\nu}(z_{13}z_{23}+\nu z_{14}z_{24})z_{34}\geqslant 0,\end{aligned} \tag{5}$$

where

$$\nu=\mu^2=\frac{\rho_{11}\rho_{44}}{\rho_{22}\rho_{33}}, \tag{6}$$

being the only information needed, at this stage, concerning the diagonal entries of ρ. (It is interesting to contrast the role of our variable ν, as it pertains to the determination of entanglement, with the rather different roles played by the *concurrence* and *negativity* [31, 32].) We have vacillated between the use of ν and μ as our principal variable in our two previous studies [9, 33]. In section 7, we will revert to the use of μ, as it appears that its use can avoid the appearances of square roots, which, it is our impression, at least, can impede certain Mathematica computations.

1.1.1. Reduction of dimensionality. Thus, the Bloore parameterization is evidently even further convenient here, in reducing the apparent dimensionality of the separable volume problem. That is, we now have to essentially consider only the separability variable ν rather than *three* independent (variable) diagonal entries. (This supplementary feature had not been commented upon by Bloore, as he discussed only 2×2 and 3×3 density matrices, and also, obviously, since the Peres-Horodecki separability condition had not yet been formulated in 1976.) The (*two* variable—ν_1, ν_2) analogue of (6) in the 6×6 (qubit–*qutrit*) case will be discussed and implemented in section 3. Additionally still, we find a *four*-variable counterpart in the 9×9 qutrit–qutrit instance (section 4), and *three*-variable counterparts in two sets of qubit–qubit–qubit analyses (sections 5 and 6). (The question of whether any or all of these several ratio variables are themselves *observables* would seem to be of some interest.) It certainly appears to us that in the qubit–qutrit case (section 3 and 10.1) the two associated ratio variables (ν_1, ν_2) importantly merge or coalesce into the simple product $\eta=\nu_1\nu_2$ for all analytical purposes. (*Products* of ratio variable do also appear in the limited number of still higher dimensional analyses we report below, so perhaps some similar merging or coalescing takes place in those settings, as well.)

In [9, equations (3)–(5)], we expressed the conditions (found through application of the 'cylindrical algebraic decomposition' [34]) that—in terms of the Bloore variables z_{ij}'s—an arbitrary nine-dimensional 4×4 real density matrix ρ must fulfil. These took the form

$$z_{12},z_{13},z_{14}\in[-1,1],z_{23}\in\left[Z_{23}^-,Z_{23}^+\right],z_{24}\in\left[Z_{24}^-,Z_{24}^+\right],z_{34}\in\left[Z_{34}^-,Z_{34}^+\right], \tag{7}$$

where

$$\begin{aligned}Z_{23}^{\pm}&=z_{12}z_{13}\pm\sqrt{1-z_{12}^2}\sqrt{1-z_{13}^2},\qquad Z_{24}^{\pm}=z_{12}z_{14}\pm\sqrt{1-z_{12}^2}\sqrt{1-z_{14}^2},\\ Z_{34}^{\pm}&=\frac{z_{13}z_{14}-z_{12}z_{14}z_{23}-z_{12}z_{13}z_{24}+z_{23}z_{24}\pm s}{1-z_{12}^2},\end{aligned} \tag{8}$$

and

$$s=\sqrt{-1+z_{12}^2+z_{13}^2-2z_{12}z_{13}z_{23}+z_{23}^2}\sqrt{-1+z_{12}^2+z_{14}^2-2z_{12}z_{14}z_{24}+z_{24}^2}. \tag{9}$$

1.1.2. Possible transformations of the z_{ij}'s. In his noteworthy paper, Bloore also presented [10, sections 6,7], a quite interesting discussion of the 'spheroidal' geometry induced by his parameterization. This strongly suggests that it might prove useful to reparameterize the z_{ij} variables in terms of spheroidal-type coordinates. Following the argument of Bloore—that is, performing rotations of the (z_{13}, z_{23}) and (z_{14}, z_{24}) vectors by $\frac{\pi}{4}$ and recognizing that each pair of so-transformed variables lay in ellipses with axes of length $\sqrt{1 \pm z_{12}}$—we were able to substantially simply the forms of the feasibility conditions (7)–(9).

Using the set of transformations (having a Jacobian equal to $\frac{(1-z_{12}^2)\gamma_1}{2\gamma_2}$)

$$\begin{aligned}
z_{13} &\to \frac{(\sqrt{1-z_{12}}\cos(\theta_1)+\sin(\theta_1)\sqrt{z_{12}+1})\sqrt{\gamma_1\gamma_2+1}}{\sqrt{2}},\\
z_{23} &\to \frac{(\sin(\theta_1)\sqrt{z_{12}+1}-\cos(\theta_1)\sqrt{1-z_{12}})\sqrt{\gamma_1\gamma_2+1}}{\sqrt{2}},\\
z_{14} &\to \frac{(\sqrt{1-z_{12}}\cos(\theta_2)+\sin(\theta_2)\sqrt{z_{12}+1})\sqrt{\gamma_1+\gamma_2}}{\sqrt{2}\sqrt{\gamma_2}},\\
z_{24} &\to \frac{(\sin(\theta_2)\sqrt{z_{12}+1}-\cos(\theta_2)\sqrt{1-z_{12}})\sqrt{\gamma_1+\gamma_2}}{\sqrt{2}\sqrt{\gamma_2}},\\
z_{34} &\to Z_{34}-\frac{\cos(\theta_1-\theta_2)\sqrt{\gamma_1+\gamma_2}\sqrt{\gamma_1\gamma_2+1}}{\sqrt{\gamma_2}},
\end{aligned} \tag{10}$$

one is able to replace conditions (7)–(9) that the real two-qubit density matrix ρ—given by (1)—must fulfil by

$$\gamma_1 \in [0,1];\quad \gamma_2 \in \left[\gamma_1, \frac{1}{\gamma_1}\right];\quad Z_{34} \in [-\gamma_1, \gamma_1];\quad z_{12} \in [-1,1];\quad \theta_1, \theta_2 \in [0, 2\pi]. \tag{11}$$

We developed this set of transformations at a rather late stage of the research reported here, and presently have no indications that are of any special aid in regard to the particular difficulties/challenges posed by the HS *separability*-probability question. So, the qubit–qubit results reported below (section 2) do rely essentially upon the conditions (7)–(9) and the original parameterization in terms of the z_{ij}'s of Bloore.

Another *very* interesting simplifying parameterization—expressed in terms of *correlations* and *partial correlations*—can be found in the statistical/mathematical literature [25, 35–38]. (In fact, the Bloore parameterization can be readily seen—in retrospect—to be simply a way of decomposing a density matrix into a *correlation matrix* (cf [39]) plus its diagonal entries.) But this too seems to have no particular enhanced value in analyzing partial transposes. (The cited literature also appears to be highly relevant to the problem of the *random* generation of density matrices.)

1.2. Previous analysis and beta function ansätze

In [9], we studied the four non-negativity conditions (as well as their counterparts—having completely parallel cancelation and univariate function properties—in the 15-dimensional case of 4×4 density matrices with, in general, *complex* entries) using *numerical* (primarily quasi-Monte Carlo integration) methods. We found a close fit to the function ([9], figures 3, 4),

$$\mathcal{S}_{\text{real}}^{\text{approx}}(\nu) = \left(4 + \frac{1}{5\sqrt{2}}\right) B\left(\frac{1}{2}, \sqrt{3}\right)^8 B_\nu\left(\frac{1}{2}, \sqrt{3}\right), \tag{12}$$

entering into our formula (cf (17), (18)),

$$V_{\text{sep/real}}^{\text{HS}} = 2\int_0^1 \mathcal{J}_{\text{real}}(\nu)\mathcal{S}_{\text{real}}(\nu)\,\mathrm{d}\nu = \int_0^\infty \mathcal{J}_{\text{real}}(\nu)\mathcal{S}_{\text{real}}(\nu)\,\mathrm{d}\nu, \tag{13}$$

for the nine-dimensional Hilbert–Schmidt *separable* volume of the real 4×4 density matrices ([9], equation (9)). Here, B denotes the (complete) beta function, and B_ν the *incomplete* beta function [40],

$$B_\nu(a, b) = \int_0^\nu w^{a-1}(1-w)^{b-1}\,\mathrm{d}w. \tag{14}$$

Additionally ([9], equation (10)),

$$\mathcal{J}_{\text{real}}(\nu) = \frac{\nu^{3/2}(12(\nu(\nu+2)(\nu^2+14\nu+8)+1)\log(\sqrt{\nu}) - 5(5\nu^4+32\nu^3-32\nu-5))}{3780(\nu-1)^9} \tag{15}$$

is the (*apparently* highly oscillatory near $\nu = 1$ [9, figure 1]) Jacobian function resulting from the transformation to the ν variable of the Bloore Jacobian $\left(\Pi_{i=1}^4 \rho_{ii}\right)^{\frac{3}{2}}$. (A referee did indicate that the apparent oscillations vanished, when he employed a Maple program using 50 digits of precision. (Only in the latest Version 6 of Mathematica is a comparable plot feasible.) Also, perhaps, we should refer to $\mathcal{J}_{\text{real}}(\nu)$ as a *marginal* Jacobian, since it is the result of the integration of a *three*-dimensional Jacobian function over two, say ρ_{11} and ρ_{22}, variables.)

In the 15-dimensional *complex* two-qubit case, we found that the function

$$S_{\text{complex}}^{\text{approx}}(\nu) = \left(\frac{100\,000\,000}{2\sqrt[3]{2} + \frac{10^{3/4}}{3^{2/3}}}\right) B\left(\frac{2\sqrt{6}}{5}, \frac{3}{\sqrt{2}}\right)^{14} B_\nu\left(\frac{2\sqrt{6}}{5}, \frac{3}{\sqrt{2}}\right), \tag{16}$$

provided a close fit to our numerical results ([18], equation (14)).

1.3. Research design and objectives

Although we were able to implement the three (six-variable) non-negativity conditions (2), (3) and (4) exactly in Mathematica in [9], for density matrices of the form (1), we found that additionally incorporating the fourth Peres–Horodecki (separability) one (5)—even holding ν fixed at specific values—seemed to yield a computationally intractable problem.

In light of the apparent computational intractability in obtaining *exact* results in the nine-dimensional real (and *a fortiori* 15-dimensional complex) two-qubit cases, we adjusted the research program pursued in [9]. We now sought to determine how far we would have to curtail the dimension (the number of free parameters) of the two-qubit systems in order to be able to obtain *exact* results using the same basic investigative framework. Such results—in addition to their own intrinsic interest—might help us understand those previously obtained (basically numerically) in the *full* 9-dimensional real and 15-dimensional complex cases [9] (which, retrospectively, in fact, we assert does turn out to be the case).

To pursue this lower dimensional exact stratagem, we nullified various m-subsets of the six symmetrically located off-diagonal pairs in the nine-parameter real density matrix (1), and tried to exactly implement the so-reduced non-negativity conditions (2), (3), (4) and (5)—both the first three (to obtain HS *total* volumes) and then all four jointly (to obtain HS *separable* volumes). We leave the four *diagonal* entries themselves alone in all our analyses, so if we nullify m pairs of symmetrically located off-diagonal entries, we are left in a (9-m)-dimensional setting. We consider the various combinatorially distinct scenarios individually, though it

would appear that we also could have grouped them into classes of scenarios equivalent under *local* operations, and simply analyzed a single representative member of each equivalence class.

We will be examining a number of scenarios of various dimensionalities (that is, differing numbers of variables parameterizing ρ). In all of them, we will seek to find the *univariate* function $\mathcal{S}_{\text{scenario}}(\nu)$ (our primary computational and theoretical challenge) and the constant c_{scenario}, such that

$$V^{\text{HS}}_{\text{sep/scenario}} = \int_0^\infty \mathcal{S}_{\text{scenario}}(\nu)\mathcal{J}_{\text{scenario}}(\nu)\,\mathrm{d}\nu, \tag{17}$$

and

$$V^{\text{HS}}_{\text{tot/scenario}} = c_{\text{scenario}} \int_0^\infty \mathcal{J}_{\text{scenario}}(\nu)\,\mathrm{d}\nu. \tag{18}$$

Given such a pair of volumes, one can immediately calculate the corresponding HS separability *probability*,

$$P^{\text{HS}}_{\text{sep/scenario}} = \frac{V^{\text{HS}}_{\text{sep/scenario}}}{V^{\text{HS}}_{\text{tot/scenario}}}. \tag{19}$$

Let us note that in the full 9-dimensional real and 15-dimensional complex two-qubit cases recently studied in [9], it was quite natural to expect that $\mathcal{S}_{\text{real}}(\nu) = \mathcal{S}_{\text{real}}\left(\frac{1}{\nu}\right)$ (and $\mathcal{S}_{\text{complex}}(\nu) = \mathcal{S}_{\text{complex}}(\frac{1}{\nu})$). But, here, in our *lower* dimensional scenarios, the nullification of entries that we employ, breaks symmetry (duality), so we can not realistically expect such a reciprocity property to hold, in general. Consequently, we adopt the more general, broader formula in (13) as our working formula (17).

We now embark upon a series of multifarious lower dimensional analyses, first for qubit–qubit and then qubit–qutrit, qutrit–qutrit and qubit–qubit–qubit systems. These will prove useful—as was our original hope—in developing approaches to higher dimensional analyses, presently out of the reach of exact computer analyses.

2. Qubit–qubit analyses

To begin, let us make the simple observation that since the partial transposition operation on a 4×4 density matrix interchanges only the (1, 4) and (2, 3) entries (and the (4, 1) and (3, 2) entries), any scenario which does not involve at least one of these entries must only yield separable states.

2.1. Five nullified pairs of off-diagonal entries—six scenarios

2.1.1. Four-dimensional real case—$P^{\text{HS}}_{\text{sep}} = \frac{3\pi}{16}$. There are, of course, six ways of nullifying *five* of the six off-diagonal pairs of entries of ρ. Of these, only two of the six yield any non-separable (entangled) states. In the four trivial (fully separable) scenarios, the lower dimensional counterpart to $\mathcal{S}_{\text{real}}(\nu)$ was of the form $\mathcal{S}_{\text{scenario}}(\nu) = c_{\text{scenario}} = 2$.

In one of the two non-trivial scenarios, having the (2, 3) and (3, 2) pair of entries of ρ left intact (not nullified), the separability function was

$$\mathcal{S}_{[(2,3)]}(\nu) = \begin{cases} 2\sqrt{\nu} & 0 \leqslant \nu \leqslant 1 \\ 2 & \nu > 1. \end{cases} \tag{20}$$

(It is of interest to note that $B_\nu\left(\frac{1}{2}, 1\right) = 2\sqrt{\nu}$, while in [9], we had conjectured that $\mathcal{S}_{\text{real}}(\nu)$ was proportional to $B_\nu\left(\frac{1}{2}, \sqrt{3}\right)$.)

In the other non-trivial scenario, with the (1,4) and (4,1) pair being the one not nullified, the separability function was—in a dual manner (mapping $f(\nu)$ for $\nu \in [0, 1]$ into $f\left(\frac{1}{\nu}\right)$ for $\nu \in [1, \infty]$)—equal to

$$\mathcal{S}_{[(1,4)]}(\nu) = \begin{cases} 2 & 0 \leqslant \nu \leqslant 1 \\ \dfrac{2}{\sqrt{\nu}} & \nu > 1. \end{cases} \tag{21}$$

In both of these scenarios (having $c_{\text{scenario}} = 2$) for the total (separable and non-separable) HS volume, we obtained $V_{\text{tot}}^{\text{HS}} = \frac{\pi}{48} \approx 0.065\,4498$ and $V_{\text{sep}}^{\text{HS}} = \frac{\pi^2}{256} \approx 0.038\,5531$. The corresponding HS separability probability for the two non-trivial (dual) scenarios is, then, $\frac{3\pi}{16} \approx 0.589\,049$.

2.1.2. Five-dimensional complex case—$P_{\text{sep}}^{\text{HS}} = \frac{1}{3}$. Now, we allow the single non-nullified pair of symmetrically located entries to be *complex* in nature (so, obviously we have five variables/parameters—that is, including the three diagonal variables—*in toto* to consider, rather than four).

Again, we have only the same two scenarios (of the six combinatorially possible) being separably non-trivial. Based on the (2, 3) and (3, 2) pair of entries, the relevant function (with the slight change of notation to indicate complex entries) was

$$\mathcal{S}_{[(2,3)]}(\nu) = \begin{cases} \pi\,\nu & 0 \leqslant \nu \leqslant 1 \\ \pi & \nu > 1 \end{cases} \tag{22}$$

and, dually,

$$\mathcal{S}_{[(1,4)]}(\nu) = \begin{cases} \pi & 0 \leqslant \nu \leqslant 1 \\ \dfrac{\pi}{\nu} & \nu > 1. \end{cases} \tag{23}$$

So, the function $\sqrt{\nu}$, which appeared (20) and (21) in the corresponding scenarios restricted to real entries, is replaced by ν itself in the complex counterpart. (We note that $B_\nu(1, 1) = \nu$.)

For both of these complex scenarios, we had $V_{\text{tot}}^{\text{HS}} = \frac{\pi}{120}$ and $V_{\text{sep}}^{\text{HS}} = \frac{\pi}{360}$, for a particularly simple HS separability probability of $\frac{1}{3}$.

2.1.3. Seven-dimensional quaternionic case—$P_{\text{sep}}^{\text{HS}} = \frac{1}{10}$. Here we allow the single pair of non-null off-diagonal entries to be *quaternionic* in nature [41, 42] ([43], section IV). We found

$$\mathcal{S}_{[(2,3)]}(\nu) = \begin{cases} \dfrac{\pi^2\nu^2}{2} & 0 \leqslant \nu \leqslant 1 \\ \dfrac{\pi^2}{2} & \nu > 1 \end{cases} \tag{24}$$

and, dually,

$$\mathcal{S}_{[(1,4)]}(\nu) = \begin{cases} \dfrac{\pi^2}{2} & 0 \leqslant \nu \leqslant 1 \\ \dfrac{\pi^2}{2\nu^2} & \nu > 1. \end{cases} \tag{25}$$

(We note that $B_\nu(2, 1) = \frac{\nu^2}{2}$.) For both scenarios, we had $V_{\text{tot}}^{\text{HS}} = \frac{\pi^2}{2520}$, $V_{\text{sep}}^{\text{HS}} = \frac{\pi^2}{25200}$, giving us $P_{\text{sep}}^{\text{HS}} = \frac{1}{10}$—which is the *smallest* separability probability we will report in this entire paper.

So, in our first set of simple ($m = 5$) scenarios, we observe a decrease in the probabilities of separability from the real to the complex to the quaternionic case, as well as a progression from $\sqrt{\nu}$ to ν to ν^2 in the functional forms occurring in the corresponding HS separability probability functions.

2.1.4. Relevance of Dyson indices. The exponents of ν in the real–complex-quaternionic progression in the immediately preceding $m = 5$ analyses, that is $\frac{1}{2}, 1, 2$ bear an evident elementary relation to the *Dyson indices* [11], $\beta = 1, 2, 4$, corresponding to the Gaussian orthogonal, unitary and symplectic ensembles [44]. (Further, many of the additional scenarios studied below—also in the non-qubit–qubit analyses—will have explicit occurrences in the corresponding separability functions of $\sqrt{\nu}$ for real entries and ν for complex entries. Of course, use of $\mu = \sqrt{\nu}$ as our principal variable would give the Dyson series itself, rather than one-half of it.) We note that the foundational work of Życzkowski and Sommers [1]) in computing the HS (separable *plus* nonseparable) volumes itself relies strongly on random matrix theory (in particular, the Laguerre ensemble). Their formula for a certain generalized (Hall) normalization constant ([1], equation (4.1)), for instance, contains a dummy variable β which equals 1 in the real case and 2 in the complex case. In their concluding remarks, they write: 'these explicit results may be applied for estimation of the volume of the set of *entangled* (emphasis added) states .... It is also likely that some of the integrals obtained in this work will be useful in such investigations' ([1], p 10125).

Of course, random matrix theory is framed in terms of the eigenvalues and eigenvectors of random matrices—which do not appear explicitly in the Bloore parameterization—so, it is not altogether transparent in what manner one might proceed further to relate the two areas. (But for the $m = 5$ highly sparse density matrices for this set of scenarios, one can explicitly transform between the eigenvalues and the Bloore parameters.)

2.2. Four nullified pairs of off-diagonal entries—15 scenarios

2.2.1. Five-dimensional real case—$P_{\text{sep}}^{\text{HS}} = \frac{5}{8}; \frac{16}{3\pi^2}$. Here, there are fifteen possible scenarios, all with $V_{\text{tot}}^{\text{HS}} = \frac{\pi^2}{480}$. Six of them are trivial (separability probabilities of 1), in which c_{scenario} is either π (scenarios [(1,2), (1,3)], [(1,2), (2,4)], [(1,3), (3,4)] and [(2,4), (3,4)]) or 4 (scenarios [(1,2), (3,4)] and [(1,3), (2,4)]). Eight of the nine non-trivial scenarios all have—similarly to the four-dimensional analyses (section 2.1.1)—separability functions $\mathcal{S}(\nu)$ either of the form

$$\mathcal{S}_{\text{scenario}}(\nu) = \begin{cases} \pi\sqrt{\nu} & 0 \leqslant \nu \leqslant 1 \\ \pi & \nu > 1, \end{cases} \tag{26}$$

(for scenarios [(1,2), (2,3)], [(1,3), (2,3)], [(2,3), (2,4)] and [(2,3), (3,4)]) or, dually,

$$\mathcal{S}_{\text{scenario}}(\nu) = \begin{cases} \pi & 0 \leqslant \nu \leqslant 1 \\ \dfrac{\pi}{\sqrt{\nu}} & \nu > 1 \end{cases} \tag{27}$$

(for scenarios [(1,2), (1,4)], [(1,3), (1,4)], [(1,4), (2,4)] and [(1,4), (3,4)]). The corresponding HS separability probabilities, for *all* eight of these non-trivial scenarios, are equal to $\frac{5}{8} = 0.625$. This result was, in all the eight cases, computed by taking the ratio of $V_{\text{sep}}^{\text{HS}} = \frac{\pi^2}{768}$ to $V_{\text{tot}}^{\text{HS}} = \frac{\pi^2}{480}$.

In the remaining (ninth) non-trivially entangled case—based on the non-nullified dyad [(1,4),(2,3)]—we have, taking the ratio of $V_{\text{sep}}^{\text{HS}} = \frac{1}{90}$ to $V_{\text{tot}}^{\text{HS}} = \frac{\pi^2}{480}$, a quite different Hilbert–Schmidt separability probability of $\frac{16}{3\pi^2} \approx 0.54038$. This isolated scenario (with $c_{\text{scenario}} = 4$) can also be distinguished from the other eight partially entangled scenarios, in that it is the only one for which entanglement occurs for *both* $\nu < 1$ and $\nu > 1$. We have

$$\mathcal{S}_{[(1,4),(2,3)]}(\nu) = \begin{cases} 4\sqrt{\nu} & 0 \leqslant \nu \leqslant 1 \\ \dfrac{4}{\sqrt{\nu}} & \nu > 1. \end{cases} \tag{28}$$

By way of illustration, in this specific case, we have the scenario-specific marginal Jacobian function

$$\mathcal{J}_{[(1,4),(2,3)]}(\nu) = -\frac{\sqrt{\nu}(-3\nu^2 + (\nu(\nu+4)+1)\log(\nu)+3)}{30(\nu-1)^5}. \tag{29}$$

2.2.2. Six-dimensional mixed (real and complex) case —$P_{\rm sep}^{\rm HS} = \frac{105\pi}{512}; \frac{135\pi}{1024}; \frac{3}{8}$. Here, we again nullify all but two of the off-diagonal entries ($m = 4$) of ρ, but allow the *first* of the two non-nullified entries to be *complex* in nature. Making (apparently necessary) use of the circular/trigonometric transformation $\rho_{11} = r^2 \sin\theta^2$, $\rho_{22} = r^2 \cos\theta^2$, we were able to obtain an interesting variety of exact results. One of these takes the form,

$$\mathcal{S}_{[(1\tilde{,}2),(1,4)]}(\nu) = \mathcal{S}_{[(1\tilde{,}3),(1,4)]}(\nu) = \left\{\left\{\frac{4\pi}{3}, 0 \leqslant \nu \leqslant 1\right\} \qquad \left\{\frac{4\pi}{3\sqrt{\nu}}, \nu > 1\right\}\right. . \tag{30}$$

Now, we have $V_{\rm tot}^{\rm HS} = \frac{\pi^2}{1440}$ and $V_{\rm sep}^{\rm HS} = \frac{7\pi^3}{49152}$, so $P_{\rm sep}^{\rm HS} = \frac{105\pi}{512} \approx 0.644272$. The two dual scenarios—having the same three results—are $[(1\tilde{,}2), (2, 3)]$ and $[(1\tilde{,}3), (2, 3)]$.

Additionally, we have an isolated scenario,

$$\mathcal{S}_{[(1\tilde{,}4),(2,3)]}(\nu) = \left\{\{2\pi\sqrt{\nu}, 0 \leqslant \nu \leqslant 1\} \qquad \left\{\frac{2\pi}{\nu}, \nu > 1\right\}\right., \tag{31}$$

for which, $V_{\rm tot}^{\rm HS} = \frac{\pi^2}{1440}$ and $V_{\rm sep}^{\rm HS} = \frac{3\pi^3}{32768}$, so $P_{\rm sep}^{\rm HS} = \frac{135\pi}{1024} \approx 0.414175$. (Note the presence of *both* $\sqrt{\nu}$ and ν in (31)—apparently related to the mixed (real and complex) nature of this scenario (cf (34)).)

Further,

$$\mathcal{S}_{[(1\tilde{,}4),(2,4)]}(\nu) = \mathcal{S}_{[(1\tilde{,}4),(3,4)]}(\nu) = \left\{\left\{\frac{4\pi}{3}, 0 \leqslant \nu \leqslant 1\right\} \qquad \left\{\frac{4\pi}{3\nu}, \nu > 1\right\}\right., \tag{32}$$

the dual scenarios being $[(2\tilde{,}3), (2, 4)]$ and $[(2\tilde{,}3), (3, 4)]$. For all four of these scenarios, $V_{\rm tot}^{\rm HS} = \frac{\pi^2}{1440}$ and $V_{\rm sep}^{\rm HS} = \frac{\pi^2}{3840}$, so $P_{\rm sep}^{\rm HS} = \frac{3}{8} = 0.375$.

2.2.3. Seven-dimensional complex case—$P_{\rm sep}^{\rm HS} = \frac{2}{5}$. Here, in an $m = 4$ setting, we nullify four of the six off-diagonal pairs of the 4×4 density matrix, allowing the remaining two pairs *both* to be complex. We have (again observing a shift from $\sqrt{\nu}$ in the real case to ν in the complex case)

$$\mathcal{S}_{[(1\tilde{,}2),(1\tilde{,}4)]}(\nu) = \mathcal{S}_{[(1\tilde{,}3),(1\tilde{,}4)]}(\nu) = \mathcal{S}_{[(1\tilde{,}4),(2\tilde{,}4)]}(\nu) = \mathcal{S}_{[(1\tilde{,}4),(3\tilde{,}4)]}(\nu) = \begin{cases} \dfrac{\pi^2}{2} & 0 \leqslant \nu \leqslant 1 \\ \dfrac{\pi^2}{2\nu} & \nu > 1. \end{cases} \tag{33}$$

Since $V_{\rm tot}^{\rm HS} = \frac{\pi^2}{5040}$ and $V_{\rm sep}^{\rm HS} = \frac{\pi^2}{12600}$, we have $P_{\rm sep}^{\rm HS} = \frac{2}{5} = 0.4$. We have the same three outcomes for the four dual scenarios $[(1\tilde{,}2), (2\tilde{,}3)]$, $[(1\tilde{,}3), (2\tilde{,}3)]$, $[(2\tilde{,}3), (2\tilde{,}4)]$ and $[(2\tilde{,}3), (3\tilde{,}4)]$, as well as—rather remarkably—for the (again isolated (cf (31))) scenario $[(1\tilde{,}4), (2\tilde{,}3)]$, having the (somewhat different) separability function (manifesting entanglement for both $\nu < 1$ and $\nu > 1$),

$$\mathcal{S}_{[(1\tilde{,}4),(2\tilde{,}3)]}(\nu) = \begin{cases} \pi^2\nu & 0 \leqslant \nu \leqslant 1 \\ \dfrac{\pi^2}{\nu} & \nu > 1. \end{cases} \tag{34}$$

(However, $c_{\text{scenario}} = \pi^2$ for this isolated scenario, while it equals $\frac{\pi^2}{2}$ for the other eight.) The remaining six (fully separable) scenarios (of the fifteen possible) simply have $P_{\text{sep}}^{\text{HS}} = 1$.

2.2.4. Eight-dimensional mixed (real and quaternionic) case. We report here that

$$c_{\widetilde{[(1,2),(1,4)]}} = \frac{8\pi^2}{15}, \qquad c_{[(1,2),\widetilde{(1,4)}]} = 32, \tag{35}$$

where as before the wide tilde notation denotes the quaternionic off-diagonal entry.

2.3. Three nullified pairs of off-diagonal entries—20 scenarios

2.3.1. Six-dimensional real case—$P_{\text{sep}}^{\text{HS}} = 2 - \frac{435\pi}{1024}$. Here ($m = 3$), there are 20 possible scenarios—nullifying *triads* of off-diagonal pairs in ρ. Of these 20, there are 4 totally separable scenarios—corresponding to the non-nullified triads [(1,2), (1,3), (2,4)], [(1,2), (1,3), (3,4)], [(1,2), (2,4), (3,4)] and [(1,3), (2,4), (3,4)]—with $c_{\text{scenario}} = \frac{\pi^2}{2}$ and $V_{\text{tot}}^{\text{HS}} = V_{\text{sep}}^{\text{HS}} = \frac{\pi^3}{5760}$. To proceed further in this six-dimensional case—in which we began to encounter some computational difficulties—we sought, again, to enforce the four non-negativity conditions (2), (3), (4) and (5), but only after setting ν to specific values, rather than allowing ν to vary. We chose the nine values $\nu = \frac{1}{5}, \frac{2}{5}, \frac{3}{5}, \frac{4}{5}$, 1, 2, 3, 4 and 5. Two of the scenarios (with the triads [(1,2), (2,3), (3,4)] and [(1,3),(2,3),(2,4)]) could, then, be seen to fit unequivocally into our earlier observed predominant pattern, having the piecewise separability function,

$$\mathcal{S}_{[(1,2),(2,3),(3,4)]}(\nu) = \mathcal{S}_{[(1,3),(2,3),(2,4)]}(\nu) = \begin{cases} \dfrac{\pi^2\sqrt{\nu}}{2} & 0 \leqslant \nu \leqslant 1 \\ \dfrac{\pi^2}{2} & \nu > 1. \end{cases} \tag{36}$$

We, then, computed for these two scenarios that $V_{\text{tot}}^{\text{HS}} = \frac{\pi^3}{5760} \approx 0.00538303$ and (again making use of the transformation $\rho_{11} = r^2 \sin\theta^2$, $\rho_{22} = r^2 \cos\theta^2$) that $V_{\text{sep}}^{\text{HS}} = 2\left(\frac{\pi^3}{5760} - \frac{29\pi^4}{786432}\right) \approx 0.00358207$. This gives us $P_{\text{sep}}^{\text{HS}} = 2 - \frac{435\pi}{1024} \approx 0.665437$. For two dual cases, we have the same volumes and separability probability and, now, the piecewise separability function,

$$\mathcal{S}_{[(1,2),(1,4),(3,4)]}(\nu) = \mathcal{S}_{[(1,3),(1,4),(2,4)]}(\nu) = \begin{cases} \dfrac{\pi^2}{2} & 0 \leqslant \nu \leqslant 1 \\ \dfrac{\pi^2}{2\sqrt{\nu}} & \nu > 1. \end{cases} \tag{37}$$

We have not, to this point, been able to explicitly and succinctly characterize the functions $\mathcal{S}_{\text{scenario}}(\nu)$ for non-trivial fully real $m = 3$ scenarios other than the dual pair (36) and (37).

In all the separably non-trivial scenarios so far presented and discussed, we have had the relationship $\mathcal{S}_{\text{scenario}}(1) = c_{\text{scenario}}$. However, in our present $m = 3$ setting (three pairs of nullified off-diagonal entries), we have situations in which $\mathcal{S}_{\text{scenario}}(1) < c_{\text{scenario}}$. The values of c_{scenario} in the sixteen non-trivial fully real $m = 3$ scenarios are either $\frac{\pi^2}{2} \approx 4.9348$ (12 occurrences) or $\frac{4\pi}{3} \approx 4.18879$ (four occurrences—[(1,2), (1,3), (1,4)], [(1,2), (2,3), (2,4)], [(1,3), (2,3), (3,4)] and [(1,4), (2,4), (3,4)]). In all four of the latter ($\frac{4\pi}{3}$) occurrences, though, we have the *inequality*,

$$\mathcal{S}_{\text{scenario}}(1) = \frac{1}{24}(12 + 16\pi + 3\pi^2) \approx 3.8281 < \frac{4\pi}{3} \approx 4.18879, \tag{38}$$

as well as a parallel inequality for 4 of the 12 former $\left(\frac{\pi^2}{2}\right)$ cases. The implication of these inequalities for those eight scenarios is that at $\nu = 1$ (the value associated with the fully mixed (separable) classical state), that is, when $\rho_{11}\rho_{44} = \rho_{22}\rho_{33}$, there do exist non-separable states.

2.3.2. Seven-dimensional mixed (one complex and two real) case—$P_{\rm sep}^{\rm HS} = \frac{11}{16}$. Here, in an $m = 3$ setting, we take the first entry of the non-nullified triad to be complex and the other two real. Of the 20 possible scenarios, 4—[(1,̃2), (1, 3), (1, 4)], [(1,̃2), (2, 3), (2, 4)], [(1,̃3), (2, 3), (3, 4)] and [(1,̃4), (2, 4), (3, 4)]—had $c_{\rm scenario} = \frac{\pi^2}{2} \approx 4.9348$ and these four all had the same (lesser) value of

$$\mathcal{S}_{\rm scenario}(1) = \frac{56}{27} + \frac{\pi^2}{4} \approx 4.54148. \tag{39}$$

There were seven scenarios with $c_{\rm scenario} = \frac{16\pi}{9} \approx 5.58505$. Three of them—[(1,̃2), (1, 3), (2, 4)], [(1,̃2), (1, 4), (2, 3)] and [(1,̃3), (1, 4), (2, 3)]—had $\mathcal{S}_{\rm scenario}(1) = \frac{16\pi}{9}$ (manifesting equality), while four—[(1,̃2), (1, 3), (2, 3)], [(1,̃2), (1, 4), (2, 4)], [(1,̃3), (1, 4), (3, 4)] and [(2,̃3), (2, 4), (3, 4)]—had result (39) (manifesting inequality).

The remaining 9 of the 20 scenarios all had $c_{\rm scenario} = \mathcal{S}_{\rm scenario}(1) = \frac{2\pi^2}{3} \approx 6.57974$. For one of them, we obtained

$$\mathcal{S}_{[(1\tilde{,}2),(2,3),(3,4)]}(\nu) = \begin{cases} \dfrac{2\pi^2}{3} & \nu \geqslant 1 \\ \dfrac{2\pi^2\sqrt{\nu}}{3} & 0 < \nu < 1, \end{cases} \tag{40}$$

with associated values of $V_{\rm tot}^{\rm HS} = \frac{\pi^3}{20160}$, $V_{\rm sep}^{\rm HS} = \frac{11\pi^3}{322560}$ and $P_{\rm sep}^{\rm HS} = \frac{11}{16} \approx 0.6875$. A dual scenario to this one that we were able to find was [(1,̃2), (1, 4), (3, 4)]. The separability functions—and, hence, separability probabilities—for the other eighteen scenarios, however, are unknown to us at present.

2.3.3. Eight-dimensional mixed (two complex and one real) case. Our sole result in this category is

$$c_{[(1\tilde{,}2),(1\tilde{,}3),(1,4)]} = \frac{8\pi^2}{15}. \tag{41}$$

2.3.4. Nine-dimensional complex case. Now, we have three off-diagonal complex entries, requiring *six* parameters for their specification. This is about the limit in the number of free off-diagonal parameters for which we might hopefully be able to determine associated separability functions.

As initial findings, we obtained

$$\mathcal{S}_{[(1\tilde{,}4),(2\tilde{,}3),(2\tilde{,}4)]}(1) = c_{[(1\tilde{,}4),(2\tilde{,}3),(2\tilde{,}4)]} = \frac{\pi^3}{4}, \tag{42}$$

and also for scenarios [(1,̃2), (1,̃4), (3,̃4)], [(1,̃3), (1,̃4), (2,̃4)] and [(1,̃4), (2,̃3), (3,̃4)], while

$$c_{[(1\tilde{,}2),(1\tilde{,}3),(1\tilde{,}4)]} = c_{[(1\tilde{,}3),(2\tilde{,}3),(3\tilde{,}4)]} = c_{[(1\tilde{,}4),(2\tilde{,}4),(3\tilde{,}4)]} = \frac{\pi^3}{6}. \tag{43}$$

2.4. Two or fewer nullified pairs of off-diagonal entries

2.4.1. Seven-dimensional real case. The [(1,2), (1,3), (2,4), (3,4)] scenario is the only fully separable one of the fifteen possible ($m = 2$). For all the other fourteen non-trivial scenarios, there are non-separable states *both* for $\nu < 1$ and $\nu > 1$. For all fifteen scenarios, we have $c_{\rm scenario} = \frac{2\pi^2}{3} \approx 6.57974$. Otherwise, we have not so far been able to extend the analyses

above to this $m = 2$ fully real case (and *a fortiori* the $m = 1$ fully real case), even to determine specific values of $\mathcal{S}_{\text{scenario}}(1)$.

2.4.2. Eight-dimensional real case. Here we have $c_{\text{scenario}} = \frac{8\pi^2}{9} \approx 8.77298$ for all the six possible (separably non-trivial) scenarios ($m = 1$). Let us note that this is, in terms of preceding values of these constants (for the successively lower dimensional fully real scenarios), $\frac{8\pi^2}{9} = \frac{4}{3}\left(\frac{2\pi^2}{3}\right)$, while $\frac{2\pi^2}{3} = \frac{4}{3}\left(\frac{\pi^2}{2}\right)$. Also, $\frac{32\pi^2}{27} = \frac{4}{3}\left(\frac{8\pi^2}{9}\right)$, the further relevance of which will be apparent in relation to our discussion of the full nine-dimensional real scenario (section 9).

3. Qubit–qutrit analyses

The cancelation property, we exploited above, of the Bloore parameterization—by which the determinant and principal minors of density matrices can be *factored* into products of (non-negative) diagonal entries and terms just involving off-diagonal parameters (z_{ij})—clearly extends to $n \times n$ density matrices. It initially appeared to us that the advantage of the parameterization in studying the two-qubit HS separability probability question would diminish if one were to examine the two-qubit separability problem for other (possibly *monotone*) metrics than the HS one (cf [8]), or even the qubit–*qutrit HS* separability probability question. But upon some further analysis, we have found that the non-negativity condition for the determinant of the partial transpose of a real 6×6 (qubit–qutrit) density matrix (cf (2)) can be expressed in terms of the corresponding z_{ij}'s and *two* ratio variables (thus, not requiring the five independent diagonal variables individually),

$$\nu_1 = \frac{\rho_{11}\rho_{55}}{\rho_{22}\rho_{44}}, \qquad \nu_2 = \frac{\rho_{22}\rho_{66}}{\rho_{33}\rho_{55}}, \tag{44}$$

rather than simply one (ν) as in the 4×4 case. (We compute the qubit–qutrit partial transpose by transposing in place the four 3×3 blocks of ρ, rather than—as we might alternatively have done—the nine 2×2 blocks.)

3.1. Fourteen nullified pairs of off-diagonal entries—15 scenarios

3.1.1. Six-dimensional real case—$P^{\text{HS}}_{\text{sep}} = \frac{3\pi}{16}$. To begin our examination of the qubit–qutrit case, we study the ($m = 14$) scenarios, in which only a single pair of real entries is left intact and all other off-diagonal pairs of the 6×6 density matrix are nullified. (We not only require that the determinant of the partial transpose of ρ be non-negative for separability to hold—as suffices in the qubit–qubit case, given that ρ itself is a density matrix [45, 46]—but also, *per* the Sylvester criterion, a nested series of principal leading minors of ρ.) We have six separably non-trivial scenarios. (For all of them, $V^{\text{HS}}_{\text{tot}} = \frac{\pi}{1440}$.)

Firstly, we have the separability function

$$\mathcal{S}^{6\times 6}_{[(1,5)]}(\nu_1) = \begin{cases} 2 & \nu_1 \leqslant 1 \\ \dfrac{2}{\sqrt{\nu_1}} & \nu_1 > 1. \end{cases} \tag{45}$$

The dual scenario to this is [(2,4)]. Further,

$$\mathcal{S}^{6\times 6}_{[(1,6)]}(\nu_1, \nu_2) = \begin{cases} 2 & \nu_1\nu_2 \leqslant 1 \\ \dfrac{2}{\sqrt{\nu_1\nu_2}} & \nu_1\nu_2 > 1, \end{cases} \tag{46}$$

with the dual scenario here being [(3,4)]. Finally,

$$\mathcal{S}^{6\times 6}_{[(2,6)]}(\nu_2) = \begin{cases} 2 & \nu_2 \leqslant 1 \\ \dfrac{2}{\sqrt{\nu_2}} & \nu_2 > 1, \end{cases} \tag{47}$$

having the dual [(3,5)].

The remaining nine possible scenarios—the same as their complex counterparts in the immediate next analysis—are all fully separable in character.

We have found that $V^{\rm HS}_{\rm sep} = \frac{\pi^2}{7680}$ for the six non-trivially separable scenarios here, so $P^{\rm HS}_{\rm sep} = \frac{3\pi}{16} \approx 0.589\,049$, as in the qubit–qubit analogous case (section 2.1.1).

3.1.2. Seven-dimensional complex case—$P^{\rm HS}_{\rm sep} = \frac{1}{3}$. Now, we allow the single non-nullified pair of off-diagonal entries to be complex in nature (the two paired entries, of course, being complex conjugates of one another). ($V^{\rm HS}_{\rm tot} = \frac{\pi}{5040}$ for this series of fifteen scenarios.) Then, we have (its dual being $[(2,\tilde{}\,4)]$)

$$\mathcal{S}^{6\times 6}_{[(1,\tilde{}\,5)]}(\nu_1) = \begin{cases} \pi & \nu_1 \leqslant 1 \\ \dfrac{\pi}{\nu_1} & \nu_1 > 1. \end{cases} \tag{48}$$

Further, we have (with the dual $[(3,\tilde{}\,4)]$)

$$\mathcal{S}^{6\times 6}_{[(1,\tilde{}\,6)]}(\nu_1, \nu_2) = \begin{cases} \pi & \nu_1\nu_2 \leqslant 1 \\ \dfrac{\pi}{\nu_1\nu_2} & \nu_1\nu_2 > 1 \end{cases} \tag{49}$$

and (its dual being $[(3,\tilde{}\,5)]$),

$$\mathcal{S}^{6\times 6}_{[(2,\tilde{}\,6)]}(\nu_2) = \begin{cases} \pi & \nu_2 \leqslant 1 \\ \dfrac{\pi}{\nu_2} & \nu_2 > 1. \end{cases} \tag{50}$$

For all six of these scenarios, $V_{\rm sep} = \frac{\pi}{15120}$, so $P^{\rm sep}_{\rm HS} = \frac{1}{3}$.

3.2. Thirteen nullified pairs of off-diagonal entries—105 scenarios

3.2.1. Seven-dimensional real case—$P^{\rm HS}_{\rm sep} = \frac{5}{8}; \frac{5}{16}; \frac{3\pi}{32}; \frac{16}{3\pi^2}$. Continuing along similar lines ($m = 13$), we have 105 combinatorially distinct possible scenarios. Among the separably non-trivial scenarios, we have

$$\mathcal{S}^{6\times 6}_{[(1,2),(1,5)]}(\nu_1) = \mathcal{S}^{6\times 6}_{[(1,4),(1,5)]}(\nu_1) = \begin{cases} \pi & \nu_1 \leqslant 1 \\ \dfrac{\pi}{\sqrt{\nu_1}} & \nu_1 > 1, \end{cases} \tag{51}$$

(duals being [(1,2),(2,4)] and [(1,4),(2,4)]). We computed $V^{\rm HS}_{\rm tot} = \frac{\pi^2}{20\,610}$, $V^{\rm HS}_{\rm sep} = \frac{\pi^2}{32\,256}$, so $P^{\rm HS}_{\rm sep} = \frac{5}{8} = 0.625$ for these scenarios.

Also

$$\mathcal{S}^{6\times 6}_{[(1,3),(1,6)]}(\nu_1, \nu_2) = \mathcal{S}^{6\times 6}_{[(1,4),(1,6)]}(\nu_1, \nu_2) = \begin{cases} \pi & \nu_1\nu_2 < 1 \\ \dfrac{\pi}{\sqrt{\nu_1}\sqrt{\nu_2}} & \nu_1\nu_2 \geqslant 1. \end{cases} \tag{52}$$

We, then, have $V^{\rm HS}_{\rm tot} = \frac{\pi^2}{20\,610}$, $V^{\rm HS}_{\rm sep} = \frac{\pi^2}{64\,512}$, so $P^{\rm HS}_{\rm sep} = \frac{5}{16} = 0.3125$.

Additionally,

$$\mathcal{S}^{6\times 6}_{[(1,4),(2,6)]}(\nu_2) = \begin{cases} 4 & \nu_2 \leqslant 1 \\ \dfrac{4}{\sqrt{\nu_2}} & \nu_2 > 1. \end{cases} \tag{53}$$

For this scenario, we have $V^{\mathrm{HS}}_{\mathrm{tot}} = \frac{\pi^2}{20\,610}$, $V^{\mathrm{HS}}_{\mathrm{sep}} = \frac{\pi^2}{215\,040}$, so $P^{\mathrm{HS}}_{\mathrm{sep}} = \frac{3\pi}{32} \approx 0.294\,524$.

Further still,

$$\mathcal{S}^{6\times 6}_{[(1,5),(2,4)]}(\nu_1) = \begin{cases} \dfrac{4}{\sqrt{\nu_1}} & \nu_1 > 1 \\ 4\sqrt{\nu_1} & \nu_1 \leqslant 1. \end{cases} \tag{54}$$

For this scenario, we have $V^{\mathrm{HS}}_{\mathrm{tot}} = \frac{\pi^2}{20\,610}$, $V^{\mathrm{HS}}_{\mathrm{sep}} = \frac{1}{3780}$, so $P^{\mathrm{HS}}_{\mathrm{sep}} = \frac{16}{3\pi^2} \approx 0.54038$.

Further,

$$\mathcal{S}^{6\times 6}_{[(1,2),(2,6)]}(\nu_2) = \begin{cases} \pi & \nu_2 \leqslant 1 \\ 2\left(\cos^{-1}\left(\sqrt{1-\dfrac{1}{\nu_2}}\right) + \dfrac{\sqrt{\nu_2-1}}{\nu_2}\right) & \nu_2 > 1. \end{cases} \tag{55}$$

The separability function for [(1,3),(1,5)] is obtained from this one by replacing ν_2 by ν_1.

Also

$$\mathcal{S}^{6\times 6}_{[(1,2),(3,4)]}(\nu_1, \nu_2) = \begin{cases} \pi\sqrt{\nu_1}\sqrt{\nu_2} & \nu_1\nu_2 < 1 \\ 4\sqrt{1-\dfrac{1}{\nu_1\nu_2}} - \dfrac{2(\mathrm{i}\log\left(\frac{\sqrt{\nu_1\nu_2-1}+\mathrm{i}}{\sqrt{\nu_1}\sqrt{\nu_2}}\right)\nu_1\nu_2 + \sqrt{\nu_1\nu_2-1})}{\sqrt{\nu_1}\sqrt{\nu_2}} & \nu_1\nu_2 \geqslant 1. \end{cases} \tag{56}$$

The separability function for [(1,2),(3,5)] can be obtained from this one by setting $\nu_1 = 1$.

3.2.2. Eight-dimensional mixed (real and complex) case—$P^{\mathrm{HS}}_{\mathrm{sep}} = \frac{105\pi}{512}$. Further, we have (with $V^{\mathrm{HS}}_{\mathrm{tot}} = \frac{\pi^2}{80\,640}$ for all scenarios),

$$\mathcal{S}^{6\times 6}_{[(1,\tilde{2}),(2,4)]}(\nu_1) = \mathcal{S}^{6\times 6}_{[(1,\tilde{4}),(2,4)]}(\nu_1) = \begin{cases} \dfrac{4\pi}{3} & \nu_1 \geqslant 1 \\ \dfrac{4\pi\sqrt{\nu_1}}{3} & 0 < \nu_1 < 1. \end{cases} \tag{57}$$

Since $V^{\mathrm{HS}}_{\mathrm{sep}} = \frac{\pi^3}{393\,216}$, we have $P^{\mathrm{HS}}_{\mathrm{sep}} = \frac{105\pi}{512} \approx 0.644\,272$ for both these scenarios.

Further,

$$\mathcal{S}^{6\times 6}_{[(1,\tilde{3}),(2,4)]}(\nu_1) = \begin{cases} \dfrac{4\pi\sqrt{\nu_1}}{3} & 0 < \nu_1 \leqslant 1 \\ 2\pi - \frac{2\pi}{3\nu_1} & \nu_1 > 1 \end{cases} \tag{58}$$

and

$$\mathcal{S}^{6\times 6}_{[(1,\tilde{3}),(3,4)]}(\nu_1, \nu_2) = \mathcal{S}^{6\times 6}_{[(1,\tilde{4}),(3,4)]}(\nu_1, \nu_2) = \begin{cases} \dfrac{4\pi}{3} & \nu_1\nu_2 \geqslant 1 \\ \dfrac{4}{3}\pi\sqrt{\nu_1\nu_2} & 0 < \nu_1\nu_2 < 1. \end{cases} \tag{59}$$

Additionally,

$$\mathcal{S}^{6\times 6}_{[(2,\tilde{3}),(3,4)]}(\nu_1, \nu_2) = \begin{cases} \dfrac{4\pi}{3} & \nu_1\nu_2 \geqslant 1 \\ \dfrac{2}{3}\pi\sqrt{\nu_1\nu_2}(3-\nu_1\nu_2) & 0 < \nu_1\nu_2 < 1 \end{cases} \tag{60}$$

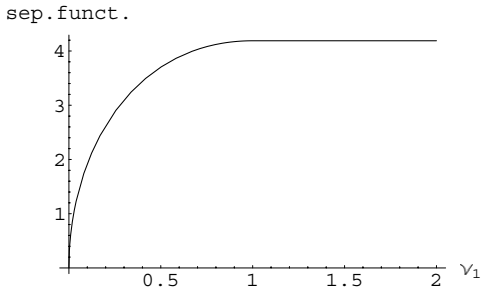

Figure 1. Plot of the separability function $S^{6\times 6}_{[(\tilde{2,3}),(2,4)]}(\nu_1)$.

and

$$\mathcal{S}^{6\times 6}_{[(\tilde{1,2}),(3,4)]}(\nu_1,\nu_2)=\begin{cases}\dfrac{4\pi}{3} & \nu_1\nu_2=1\\ \dfrac{4}{3}\pi\sqrt{\nu_1\nu_2} & 0<\nu_1\nu_2<1\\ \pi(\sqrt{\nu_1\nu_2}+2)-\dfrac{2\pi}{3\nu_1\nu_2} & \nu_1\nu_2>1.\end{cases}\tag{61}$$

We have also obtained the separability function (figure 1)

$$\mathcal{S}^{6\times 6}_{[(\tilde{2,3}),(2,4)]}(\nu_1)=\begin{cases}\dfrac{4\pi}{3} & \nu_1\geqslant 1\\ \dfrac{2}{3}\pi(3-\nu_1)\sqrt{\nu_1} & 0<\nu_1<1.\end{cases}\tag{62}$$

Of the 105 possible scenarios, 60 had $S^{6\times 6}_{\text{scenario}}(1,1)=c_{\text{scenario}}=\frac{4\pi}{3}$, 33 had $S^{6\times 6}_{\text{scenario}}(1,1)=c_{\text{scenario}}=2\pi$, and 12 (for example, $[(\tilde{3,4}),(5,6)]$) had $S^{6\times 6}_{\text{scenario}}(1,1)=\frac{4\pi}{3}<c_{\text{scenario}}=2\pi$.

3.2.3. Nine-dimensional complex case—$P^{\text{HS}}_{\text{sep}}=\frac{1}{3};\frac{2}{5}$. We have obtained the results

$$\mathcal{S}^{6\times 6}_{[(\tilde{1,2}),(\tilde{2,4})]}(\nu_1)=\mathcal{S}^{6\times 6}_{[(\tilde{1,4}),(\tilde{2,4})]}(\nu_1)=\begin{cases}\dfrac{\pi^2\nu_1}{2} & 0\leqslant\nu_1\leqslant 1\\ \dfrac{\pi^2}{2} & \nu_1>1.\end{cases}\tag{63}$$

Since $V^{\text{HS}}_{\text{tot}}=\frac{\pi^2}{362\,880}$ and $V^{\text{HS}}_{\text{sep}}=\frac{\pi^2}{907\,200}$, we have here $P^{\text{HS}}_{\text{sep}}=\frac{2}{5}=0.4$. We have the same three outcomes also based on the separability function

$$\mathcal{S}^{6\times 6}_{[(\tilde{1,4}),(\tilde{3,4})]}(\nu_1,\nu_2)=\begin{cases}\dfrac{\pi^2}{2} & \nu_1\nu_2\geqslant 1\\ \dfrac{1}{2}\pi^2\nu_1\nu_2 & \nu_1\nu_2<1.\end{cases}\tag{64}$$

Further,

$$\mathcal{S}^{6\times 6}_{[(\tilde{1,2}),(\tilde{3,4})]}(\nu_1,\nu_2)=\begin{cases}\dfrac{2\pi^2\nu_1\nu_2-\pi^2}{2\nu_1\nu_2} & \nu_1\nu_2>1\\ \dfrac{1}{2}\pi^2\nu_1\nu_2 & 0<\nu_1\nu_2\leqslant 1.\end{cases}\tag{65}$$

and

$$\mathcal{S}^{6\times 6}_{[(1,\tilde{3}),(2,\tilde{4})]}(\nu_1) = \begin{cases} \dfrac{\pi^2\nu_1}{2} & 0 < \nu_1 \leqslant 1 \\ \pi^2 - \dfrac{\pi^2}{2\nu_1} & \nu_1 > 1. \end{cases} \tag{66}$$

For both of these last two scenarios, we have $V^{\mathrm{HS}}_{\mathrm{tot}} = \frac{\pi^2}{362\,880}$ and $V^{\mathrm{HS}}_{\mathrm{sep}} = \frac{\pi^2}{362\,880}$, leading to $P^{\mathrm{HS}}_{\mathrm{sep}} = \frac{1}{3} \approx 0.33\,333$. Also, we have these same three outcomes based on the separability function

$$\mathcal{S}^{6\times 6}_{[(2,\tilde{3}),(3,\tilde{4})]}(\nu_1, \nu_2) = \begin{cases} \dfrac{\pi^2}{2} & \nu_1\nu_2 \geqslant 1 \\ \dfrac{1}{2}\pi^2\nu_1\nu_2(2 - \nu_1\nu_2) & 0 < \nu_1\nu_2 < 1. \end{cases} \tag{67}$$

Of the 105 possible scenarios—in complete parallel to those in the immediately preceding section—60 had $S^{6\times 6}_{\mathrm{scenario}}(1, 1) = c_{\mathrm{scenario}} = \frac{\pi^2}{2}$, 33 had $S^{6\times 6}_{\mathrm{scenario}}(1, 1) = c_{\mathrm{scenario}} = \pi^2$, and 12 (for example, $[(3,\tilde{4}), (5,\tilde{6})]$) had $S^{6\times 6}_{\mathrm{scenario}}(1, 1) = \frac{\pi^2}{2} < c_{\mathrm{scenario}} = \pi^2$.

Our results in this (nine-dimensional) section and the (eight-dimensional) one immediately preceding it are still incomplete with respect to various scenario-specific separability functions and, thus, the associated HS separability properties.

3.3. Twelve nullified pairs of off-diagonal entries—455 scenarios

3.3.1. Eight-dimensional real case. Now, we allow three of the off-diagonal pairs of entries to be nonzero, but also require them to be simply real. We found the separability function

$$\begin{aligned} &\mathcal{S}_{[(1,2),(1,3),(3,4)]}(\nu_1, \nu_2) = \mathcal{S}_{[(1,2),(1,4),(3,4)]}(\nu_1, \nu_2) \\ &= \begin{cases} \frac{4\pi}{3} & \frac{1}{\nu_1} = \nu_2 \wedge \nu_1 > 0 \\ \frac{4}{3}\pi\sqrt{\nu_1\nu_2} & \nu_1 > 0 \wedge \frac{1}{\nu_1} > \nu_2 \wedge \nu_2 > 0 \\ \frac{1}{3}\pi\left(3\sec^{-1}(\sqrt{\nu_1\nu_2}) + 4\sqrt{\nu_1\nu_2} + \frac{\sqrt{\nu_1\nu_2 - 1}}{\nu_1\nu_2} - 4\sqrt{\nu_1\nu_2 - 1}\right) & \nu_1 > 0 \wedge \frac{1}{\nu_1} < \nu_2. \end{cases} \end{aligned} \tag{68}$$

Also, we have

$$\begin{aligned} &\mathcal{S}_{[(1,3),(1,4),(2,4)]}(\nu_1) \\ &= \begin{cases} \dfrac{4\pi}{3} & \nu_1 = 1 \\ \dfrac{4\pi\sqrt{\nu_1}}{3} & 0 < \nu_1 < 1 \\ \dfrac{\pi\left(4\nu_1^{3/2} + \left(3\sin^{-1}\left(\sqrt{1 - \frac{1}{\nu_1}}\right) - 4\sqrt{\nu_1 - 1}\right)\nu_1 + \sqrt{\nu_1 - 1}\right)}{3\nu_1} & \nu_1 > 1. \end{cases} \end{aligned} \tag{69}$$

We note, importantly, that in all the qubit–qutrit scenarios in which ν_1 and ν_2 have both appeared in the (naively, bivariate) separability function, it has been in the *product* form $\nu_1\nu_2$ (cf section 10.1).

4. Qutrit–qutrit analyses

In the qubit–qubit (4×4 density matrix) case, we were able to express the condition (5) that the determinant of the partial transpose of ρ be non-negative in terms of *one* supplementary

variable (ν), given by (6), rather than three independent diagonal entries. Similarly, in the qubit–qutrit (6×6 density matrix) case, we could employ *two* supplementary variables (ν_1, ν_2), given by (44), rather than five independent diagonal entries.

For the qutrit–qutrit (9×9 density matrix) case, rather than eight independent diagonal entries, we found that one can employ the *four* supplementary variables

$$\nu_1 = \frac{\rho_{11}\rho_{55}}{\rho_{22}\rho_{44}}; \qquad \nu_2 = \frac{\rho_{22}\rho_{66}}{\rho_{33}\rho_{55}}; \qquad \nu_3 = \frac{\rho_{44}\rho_{88}}{\rho_{55}\rho_{77}}; \qquad \nu_4 = \frac{\rho_{55}\rho_{99}}{\rho_{66}\rho_{88}}. \tag{70}$$

4.1. Thirty-five nullified pairs of off-diagonal entries—36 scenarios

4.1.1. Ten-dimensional complex case—$P_{\rm PPT}^{\rm HS} = \frac{1}{3}; \frac{1}{6}$. Here, we nullify all but one of the 36 pairs of off-diagonal entries of the 9×9 density matrix ρ. We allow this solitary pair to be composed of complex conjugates. Since the Peres–Horodecki positive partial transposition (PPT) criterion is not sufficient to ensure separability, we accordingly modify our notation.

Our first result is

$$\mathcal{S}^{9\times 9}_{[(1\tilde{,}5)]}(\nu_1) = \begin{cases} \pi & \nu_1 \leqslant 1 \\ \dfrac{\pi}{\nu_1} & \nu_1 > 1 \end{cases} \tag{71}$$

(a dual scenario being $[(2\tilde{,}4)]$). We have $V_{\rm tot}^{\rm HS} = \frac{\pi}{3628\,800}$, $V_{\rm PPT}^{\rm HS} = \frac{\pi}{10\,886\,400}$, so $P_{\rm PPT}^{\rm HS} = \frac{1}{3}$.

The same three outcomes are obtained based on the PPT function

$$\mathcal{S}^{9\times 9}_{[(1\tilde{,}6)]}(\nu_1, \nu_2) = \begin{cases} \pi & \nu_1\nu_2 \leqslant 1 \\ \dfrac{\pi}{\nu_1\nu_2} & \nu_1\nu_2 > 1. \end{cases} \tag{72}$$

On the other hand, we have $V_{\rm tot}^{\rm HS} = \frac{\pi}{3628\,800}$, $V_{\rm PPT}^{\rm HS} = \frac{\pi}{21\,772\,800}$ and $P_{\rm PPT}^{\rm HS} = \frac{1}{6}$ based on the PPT function

$$\mathcal{S}^{9\times 9}_{[(6\tilde{,}8)]}(\nu_4) = \begin{cases} \pi & \nu_4 \geqslant 1 \\ \pi\nu_4 & 0 < \nu_4 < 1. \end{cases} \tag{73}$$

Of the 36 combinatorially possible scenarios, 13 had $P_{\rm PPT}^{\rm HS} = \frac{1}{3}$, while 4 had $P_{\rm PPT}^{\rm HS} = \frac{1}{3}$, and the remaining 19 were fully separable in nature.

4.2. Thirty-four nullified pairs of off-diagonal entries—630 scenarios

4.2.1. 12-dimensional complex case—$P_{\rm PPT}^{\rm HS} = \frac{1}{3}; \frac{7}{30}$. Since the number of combinatorially possible scenarios was so large, we randomly generated scenarios to examine.

Firstly, we found

$$\mathcal{S}^{9\times 9}_{[(1\tilde{,}4),(3\tilde{,}5)]}(\nu_2) = \begin{cases} \pi^2 & \nu_2 \geqslant 1 \\ \pi^2\nu_2 & 0 < \nu_2 < 1. \end{cases} \tag{74}$$

For this scenario, we had $V_{\rm tot}^{\rm HS} = \frac{\pi^2}{479\,001\,600}$, $V_{\rm PPT}^{\rm HS} = \frac{\pi^2}{1437\,004\,800}$, giving us $P_{\rm PPT}^{\rm HS} = \frac{1}{3}$.

Also, we found

$$\mathcal{S}^{9\times 9}_{[(2\tilde{,}9),(6\tilde{,}9)]}(\nu_2, \nu_4) = \begin{cases} \dfrac{\pi^2}{2} & \nu_2\nu_4 \leqslant 1 \\ \dfrac{\pi^2(2\nu_2\nu_4 - 1)}{2\nu_2^2\nu_4^2} & \nu_2\nu_4 > 1. \end{cases} \tag{75}$$

For this scenario, we had $V_{\rm tot}^{\rm HS} = \frac{\pi^2}{479\,001\,600}$, $V_{\rm PPT}^{\rm HS} = \frac{\pi^2}{205\,2864\,000}$, giving us $P_{\rm PPT}^{\rm HS} = \frac{7}{30} \approx 0.23333$.

5. Qubit–qubit–qubit analyses: I

For initial relative simplicity, let us regard an 8×8 density matrix ρ as a *bipartite* system, a composite of a four-level system and a two-level system. Then, we can compute the partial transposition of ρ, transposing in place its four 4×4 blocks. The non-negativity of this partial transpose can be expressed using just *three* ratio variables,

$$\nu_1 = \frac{\rho_{11}\rho_{66}}{\rho_{22}\rho_{55}}; \qquad \nu_2 = \frac{\rho_{22}\rho_{77}}{\rho_{33}\rho_{66}}; \qquad \nu_3 = \frac{\rho_{33}\rho_{88}}{\rho_{44}\rho_{77}}, \tag{76}$$

rather than seven independent diagonal entries.

5.1. Twenty-seven nullified pairs of off-diagonal entries—28 scenarios

5.1.1. Nine-dimensional complex case—$P_{\text{PPT}}^{\text{HS}} = \frac{1}{3}$. We have the PPT function

$$\mathcal{S}^{8\times 8}_{[(1,\tilde{6})]}(\nu_1) = \begin{cases} \pi & \nu_1 \leqslant 1 \\ \dfrac{\pi}{\nu_1} & \nu_1 > 1. \end{cases} \tag{77}$$

(Scenario $[(2,\tilde{5})]$ was dual to this one.) For this scenario, $V_{\text{tot}}^{\text{HS}} = \frac{\pi}{362\,880}$, $V_{\text{PPT}}^{\text{HS}} = \frac{\pi}{1088\,640}$, yielding $P_{\text{PPT}}^{\text{HS}} = \frac{1}{3}$. There were 12 scenarios, *in toto*, with precisely these three outcomes. The other 16 were all fully separable in nature.

5.2. Twenty-six nullified pairs of off-diagonal entries—378 scenarios

5.2.1. 11-dimensional complex case—$P_{\text{PPT}}^{\text{HS}} = \frac{1}{3}; \frac{1}{9}$. Again, because of the large number of possible scenarios, we chose them randomly for inspection.

Firstly, we obtained

$$\mathcal{S}^{8\times 8}_{[(3,\tilde{5}),(6,\tilde{8})]}(\nu_1, \nu_2) = \begin{cases} \pi^2 & \nu_1 > 0 \wedge \dfrac{1}{\nu_1} \leqslant \nu_2 \\ \pi^2 \nu_1 \nu_2 & \nu_1 > 0 \wedge \dfrac{1}{\nu_1} > \nu_2 \wedge \nu_2 > 0. \end{cases} \tag{78}$$

(Of course, the symbols '$\wedge$' and '$\vee$', used by Mathematica in its output, denote the logical connectives 'and' (conjunction) and 'or' (intersection) of propositions.) For this scenario, we had $V_{\text{tot}}^{\text{HS}} = \frac{\pi^2}{39\,916\,800}$, $V_{\text{PPT}}^{\text{HS}} = \frac{\pi^2}{119\,750\,400}$, giving us $P_{\text{PPT}}^{\text{HS}} = \frac{1}{3}$.

Also

$$\mathcal{S}^{8\times 8}_{[(2,\tilde{5}),(4,\tilde{7})]}(\nu_1, \nu_2) = \begin{cases} \pi^2 & \nu_1 \geqslant 1 \wedge \nu_3 \geqslant 1 \\ \pi^2 \nu_1 & 0 < \nu_1 < 1 \wedge \nu_3 \geqslant 1 \\ \pi^2 \nu_3 & \nu_1 \geqslant 1 \wedge 0 < \nu_3 < 1 \\ \pi^2 \nu_1 \nu_3 & 0 < \nu_1 < 1 \wedge 0 < \nu_3 < 1. \end{cases} \tag{79}$$

For this scenario, we had $V_{\text{tot}}^{\text{HS}} = \frac{\pi^2}{39\,916\,800}$, $V_{\text{PPT}}^{\text{HS}} = \frac{\pi^2}{359\,251\,200}$, giving us $P_{\text{PPT}}^{\text{HS}} = \frac{1}{9}$.

We also found the PPT function

$$\mathcal{S}^{8\times 8}_{[(1,\tilde{3}),(4,\tilde{7})]}(\nu_1) = \begin{cases} \dfrac{\pi^2}{2} & \nu_3 = 1 \\ \dfrac{\pi^2 \nu_3}{2} & 0 < \nu_3 < 1 \\ \pi \left(\cos^{-1}\left(\sqrt{1 - \dfrac{1}{\nu_3}} \right) - \sin^{-1}\left(\dfrac{1}{\sqrt{\nu_3}} \right) \right) \nu_3 + \pi^2 - \dfrac{\pi^2}{2\nu_3} & \nu_3 > 1. \end{cases} \tag{80}$$

6. Qubit–qubit–qubit analyses: II

Here we regard the 8×8 density matrix as a *tripartite* composite of three two-level systems, and compute the partial transpose by transposing, in place, the eight 2×2 blocks of ρ. (For *symmetric* states of three qubits, positivity of the partial transpose is *sufficient* to ensure separability [47, 48].) Again the non-negativity of the determinant could be expressed using three (different) ratio variables,

$$\nu_1 = \frac{\rho_{11}\rho_{44}}{\rho_{22}\rho_{33}}; \qquad \nu_2 = \frac{\rho_{44}\rho_{55}}{\rho_{33}\rho_{66}}; \qquad \nu_3 = \frac{\rho_{55}\rho_{88}}{\rho_{66}\rho_{77}}, \tag{81}$$

6.1. Twenty-seven nullified pairs of off-diagonal entries—28 scenarios

6.1.1. Nine-dimensional complex case—$P_{\rm PPT}^{\rm HS} = \frac{1}{3}$. There were, again, 12 of 28 scenarios with non-trivial separability properties, all with $V_{\rm tot}^{\rm HS} = \frac{\pi}{362\,880}$, $V_{\rm PPT}^{\rm HS} = \frac{\pi}{1088\,640}$, yielding $P_{\rm PPT}^{\rm HS} = \frac{1}{3}$. One of these was

$$\mathcal{S}^{8\times 8}_{[(1,\tilde{4})]}(\nu_1) = \begin{cases} \pi & \nu_1 \leqslant 1 \\ \dfrac{\pi}{\nu_1} & \nu_1 > 1. \end{cases} \tag{82}$$

6.1.2. 11-dimensional complex case—$P_{\rm PPT}^{\rm HS} = \frac{17}{60}; \frac{1}{3}$. We obtained the PPT function

$$\mathcal{S}^{8\times 8}_{[(1,\tilde{8}),(5,\tilde{7})]}(\nu_1, \nu_2, \nu_3) = \begin{cases} \dfrac{\pi^2}{2} & \dfrac{\nu_2}{\nu_1} = \nu_3 \wedge \nu_1 > 0 \wedge \nu_2 > 0 \\ \pi^2 & \nu_2 > 0 \wedge ((\nu_1 = 0 \wedge \nu_3 \geqslant 0) \vee (\nu_3 = 0 \wedge \nu_1 > 0)) \\ \dfrac{\pi^2 \nu_2}{4\nu_1\nu_3} & \nu_1 > 0 \wedge \nu_2 > 0 \wedge \dfrac{\nu_2}{\nu_1} < \nu_3 \\ \pi^2 - \dfrac{\pi^2\nu_1\nu_3}{2\nu_2} & \nu_1 > 0 \wedge \nu_2 > 0 \wedge \dfrac{\nu_2}{\nu_1} > \nu_3 \wedge \nu_3 > 0. \end{cases} \tag{83}$$

For this we had $V_{\rm tot}^{\rm HS} = \frac{\pi^2}{39\,916\,800}$, $V_{\rm PPT}^{\rm HS} = \frac{17\pi^2}{239\,500\,800}$, giving us $P_{\rm PPT}^{\rm HS} = \frac{17}{60} \approx 0.283\,333$.

Additionally,

$$\mathcal{S}^{8\times 8}_{[(1,\tilde{4}),(7,\tilde{8})]}(\nu_1) = \begin{cases} \pi^2 & \nu_1 \leqslant 1 \\ \dfrac{\pi^2}{\nu_1} & \nu_1 > 1. \end{cases} \tag{84}$$

Here, we had $V_{\rm tot}^{\rm HS} = \frac{\pi^2}{39\,916\,800}$, $V_{\rm PPT}^{\rm HS} = \frac{17\pi^2}{119\,750\,400}$, giving us $P_{\rm PPT}^{\rm HS} = \frac{1}{3}$.

Another PPT function we were able to find was

$$\mathcal{S}^{8\times 8}_{[(3,\tilde{4}),(3,\tilde{8})]}(\nu_2, \nu_3) = \begin{cases} \dfrac{\pi^2}{2} & \nu_2 > 0 \wedge (\nu_3 = \nu_2 \vee (\nu_2 > \nu_3 \wedge \nu_2 < 2\nu_3) \vee (\nu_2 \geqslant 2\nu_3 \wedge \nu_3 \geqslant 0)) \\ \dfrac{\pi^2\nu_2(2\nu_3 - \nu_2)}{2\nu_3^2} & \nu_2 > 0 \wedge \nu_2 < \nu_3. \end{cases} \tag{85}$$

7. Approximate approaches to nine-dimensional real qubit–qubit scenario

As we have earlier noted, it appears that the simultaneous computational enforcement of the four conditions (2), (3), (4) and (5) that would yield the nine-dimensional volume of the separable real two-qubit states appears presently highly intractable. But if we replace (5) by *less* strong conditions on the non-negativity of the partial transpose (ρ^T), we can achieve some form of approximation to the desired results. So, replacing (5) by the requirement (derived from a 2×2 principal minor of ρ^T) that

$$1 - \nu z_{14}^2 \geqslant 0, \tag{86}$$

we obtain the *approximate* separability function

$$S_{\text{real}}^{\text{approx}}(\nu) = \begin{cases} \dfrac{512\pi^2}{27} & 0 < \nu \leqslant 1 \\ \dfrac{256(3\pi^2\nu - \pi^2)}{27\nu^{3/2}} & \nu > 1. \end{cases} \tag{87}$$

(In the analyses in this section, we utilize the integration limits on the z_{ij}'s [9, equations (3)–(5)] yielded by the cylindrical decomposition algorithm (CAD), to reduce the dimensionalities of our constrained integrations.) This yields an *upper bound* on the separability probability of the real nine-dimensional qubit–qubit states of $\frac{1}{2} + \frac{512}{135\pi^2} \approx 0.88\,427$. We obtain the same probability if we employ instead of (86) the requirement

$$\nu - z_{23}^2 \geqslant 0, \tag{88}$$

which yields the dual function to (87), namely,

$$S_{\text{real}}^{\text{approx}}(\nu) = \begin{cases} \dfrac{512\pi^2}{27} & \nu \geqslant 1 \\ \dfrac{256}{27}\pi^2(3-\nu)\sqrt{\nu} & 0 < \nu < 1. \end{cases} \tag{89}$$

(The left-hand sides of (86) and (88) are the only two of the six 2×2 principal minors of ρ^T that are non-trivially distinct—apart from cancelable non-negative factors—from the corresponding minors of ρ itself.) The non-constant functional form in the second line of (89) will emerge again, *importantly*, in (93).

If we form a 'quasi-separability' function over $\nu \in [0, \infty]$ by piecing together the non-constant segments of (87) and (89), we can infer—using a simple symmetry, duality argument—an improved (lowered) upper bound on the HS separability probability of $\frac{1024}{135\pi^2} \approx 0.76\,854$. We can also reach such a result by noting that the two constraints (86) and (88) are independent (involve different variables), so we should just be able to multiply the corresponding functions (and then scale them by the corresponding $c_{\text{scenario}} = \frac{512\pi^2}{27}$)

8. Alternative use of Bloch parameterization

We may say, in partial summary that we have been able to obtain certain *exact* two-qubit HS separability probabilities in dimensions 7 or less, making use of the advantageous Bloore parameterization [10], but not yet in dimensions greater than 7. This, however, is considerably greater than simply the three dimensions (parameters) we were able to achieve [17] in a somewhat comparable study based on the *generalized Bloch representation* parameterization [49, 50]. In [17]—extending an approach of Jakóbczyk and Siennicki [50]—we primarily studied *two*-dimensional sections of a set of generalized Bloch vectors corresponding to $n \times n$ density matrices, for $n = 4, 6, 8, 9$ and 10. For $n > 4$, by far the most frequently recorded HS

separability (or positive partial transpose (PPT) for $n > 6$) probability was $\frac{\pi}{4} \approx 0.785\,398$. A very wide range of exact HS separability and PPT probabilities was tabulated.

Immediately below is just one of the many matrix tables (this one being numbered (5)) presented in [17] (which due to its copious results has been left simply as a preprint, rather than submitted directly to a journal). This table gives the HS separability probabilities for the qubit–qutrit case. In the first column are given the identifying numbers of a *pair* of generalized Gell–Mann matrices (generators of $SU(6)$). In the second column of (90) are shown the *number* of distinct unordered pairs of $SU(6)$ generators which share the same total (separable and nonseparable) HS volume, as well as the same separable HS volume, and consequently, identical HS separability probabilities. The third column gives us these HS total volumes, the fourth column, the HS separability probabilities and the last (fifth) column, numerical approximations to the exact probabilities (which, of course, we see—being probabilities—do not exceed the value 1). (The HS separable volumes too can be deduced from the total volume and the separability probability.)

$$\begin{pmatrix}
\{1,13\} & 48 & \frac{4}{9} & \frac{\pi}{4} & 0.785\,398 \\
\{3,11\} & 4 & \frac{8\sqrt{2}}{27} & \frac{1}{\sqrt{2}} & 0.707\,107 \\
\{3,13\} & 4 & \frac{4}{9} & \frac{5}{6} & 0.833\,333 \\
\{3,25\} & 4 & \frac{8\sqrt{2}}{27} & \frac{5}{4\sqrt{2}} & 0.883\,883 \\
\{8,13\} & 4 & \frac{2}{3} & \frac{1}{\sqrt{3}} & 0.577\,350 \\
\{8,25\} & 4 & \frac{\sqrt{2}}{3} & \sqrt{\frac{2}{3}} & 0.816\,497 \\
\{11,15\} & 4 & \frac{4\sqrt{2}\pi}{27} & \frac{1}{3}+\frac{3\sqrt{3}}{4\pi} & 0.746\,830 \\
\{11,24\} & 2 & \frac{25\sqrt{\frac{5}{2}}}{72} & \frac{2}{5}+\frac{1}{2}\sin^{-1}\left(\frac{4}{5}\right) & 0.863\,648 \\
\{13,24\} & 2 & \frac{25\sqrt{\frac{5}{2}}}{72} & \frac{8}{75}(-2+5\sqrt{5}) & 0.979\,236 \\
\{13,35\} & 4 & \frac{4\sqrt{\frac{3}{5}}}{5} & \frac{1}{12}\left(5+3\sqrt{5}\sin^{-1}\left(\frac{\sqrt{5}}{3}\right)\right) & 0.886\,838 \\
\{15,16\} & 4 & \frac{32\sqrt{2}}{81} & \frac{1}{32}(9\sqrt{3}+4\pi) & 0.879\,838 \\
\{16,24\} & 2 & \frac{25}{144}\sqrt{\frac{5}{2}}\pi & \frac{4+5\sin^{-1}\left(\frac{4}{5}\right)}{5\pi} & 0.549\,815 \\
\{20,24\} & 2 & \frac{25}{144}\sqrt{\frac{5}{2}}\pi & \frac{92+75\sin^{-1}\left(\frac{4}{5}\right)}{75\pi} & 0.685\,627 \\
\{24,25\} & 2 & \frac{25}{27\sqrt{2}} & 1-\frac{2}{5\sqrt{5}} & 0.821\,115 \\
\{24,27\} & 2 & \frac{25}{27\sqrt{2}} & \frac{92+75\cos^{-1}\left(\frac{3}{5}\right)}{80\sqrt{5}} & 0.903\,076 \\
\{25,35\} & 4 & \frac{\sqrt{3}\pi}{5} & \frac{\sqrt{5}+3\csc^{-1}\left(\frac{3}{\sqrt{5}}\right)}{3\pi} & 0.504\,975
\end{pmatrix}. \tag{90}$$

It might be of interest to address separability problems that appear to be computationally intractable in the generalized Bloch representation by transforming them into the Bloore parameterization.

9. *Full* real and complex two-qubit separability probability conjectures

The qubit–qubit results above (section 2) motivated us to reexamine previously obtained results (cf ([33], equations (12), (13))) and we would like to make the following observations

pertaining to the *full* 9-dimensional real and 15-dimensional HS separability probability issue. We have the exact results in these two cases that

$$\int_0^\infty \mathcal{J}_{\text{real}}(\nu) = 2\int_0^1 \mathcal{J}_{\text{real}}(\nu) = \frac{\pi^2}{1146\,880} \approx 8.60561 \times 10^{-6} \tag{91}$$

and

$$\int_0^\infty \mathcal{J}_{\text{complex}}(\nu) = 2\int_0^1 \mathcal{J}_{\text{complex}}(\nu) = \frac{1}{1009\,008\,000} \approx 9.91072 \times 10^{-10}. \tag{92}$$

Now, to obtain the corresponding *total* (separable plus nonseparable) HS volumes computed by Życzkowski and Sommers [1], that is, $\frac{\pi^4}{60\,480} \approx 0.001\,6106$ and $\frac{\pi^6}{851\,350\,500} \approx 1.12925 \times 10^{-6}$, one must multiply (91) and (92) by the factors of $C_{\text{real}} = \frac{512\pi^2}{27} = \frac{2^8\pi^2}{3^3} \approx 187.157$ and $C_{\text{complex}} = \frac{32\pi^6}{27} = \frac{2^5\pi^6}{3^3} \approx 1139.42$, respectively.

To most effectively compare these previously reported results with those derived above in this paper, one needs to multiply C_{real} and $\mathcal{S}_{\text{real}}(\nu)$, by $2^{-4} = \frac{1}{16}$ and in the complex case by $2^{-7} = \frac{1}{128}$. Doing so, for example, would adjust C_{real} to equal $c_{\text{real}} = \frac{32\pi^2}{27} \approx 11.6973$, which we note, in line with our previous series of calculations (section 2.4.2) is equal to $\frac{4}{3}\left(\frac{8\pi^2}{9}\right)$. (Andai [5] also computed the same volumes—up to a normalization factor—as Życzkowski and Sommers [1].) Now, our estimates from [9] are that $\mathcal{S}_{\text{real}}(1) = 114.62351 < C_{\text{real}}$ and $\mathcal{S}_{\text{complex}}(1) = 387.50809 < C_{\text{complex}}$. These results would appear—as remarked above—to be a reflection of the phenomena that there are non-separable states for both the 9- and 15-dimensional scenarios at $\nu = 1$ (the locus of the fully mixed, classical state).

Alternatively, the results in section 2.1.3, and further throughout the paper, in which we find a relation between separability functions and the Dyson indices ($\beta = 1, 2, 4$) of random matrix theory—including the frequent occurrence of $\sqrt{\nu}$ in a real scenario and ν in the corresponding complex scenario—strongly suggest that in the full ($m = 0$) 9-dimensional real and 15-dimensional complex cases scenarios, the separability function for the complex case might simply be proportional to the *square* of the separability function for the real case (and, in the quaternionic case [42], to the *fourth* power of that function).

Following such a line of thought, we were led to reexamine the numerical analyses reported in [9], in which we had formulated our beta function ansätze. In figure 2 we show the previously obtained numerical estimates of $\mathcal{S}_{\text{real}}(\nu)$ and $\mathcal{S}_{\text{complex}}(\nu)$, now both scaled (regularized) to equal 1 at $\nu = 1$, along with the similarly regularized form (termed the 'incomplete beta function ratio' [40] or, alternatively, the 'regularized incomplete beta function')

$$I_\nu\left(\nu, \tfrac{1}{2}, 2\right) = \tfrac{1}{2}(3 - \nu)\sqrt{\nu} \tag{93}$$

of the incomplete beta function, $B_\nu\left(\nu, \frac{1}{2}, 2\right) = \frac{2}{3}(3 - \nu)\sqrt{\nu})$ and $I_\nu\left(\nu, \frac{1}{2}, 2\right)^2$. (Let us make the important observation here that the functional form (93) has—up to proportionality—already occurred (although we did not immediately perceive then its beta function expression) in certain previous exact qubit–qubit analyses (89) (see also (60) (62), but also (67), for its occurrence in the qubit–qutrit context).

Figure 2 does reveal an extraordinarily good fit between the normalized numerical estimates of $\mathcal{S}_{\text{complex}}(\nu)$ and $I_\nu\left(\nu, \frac{1}{2}, 2\right)^2$, while $I_\nu\left(\nu, \frac{1}{2}, 2\right)$ itself provides a close fit to the normalized numerical estimates of $\mathcal{S}_{\text{real}}(\nu)$. (Note that $I_\nu\left(\nu, \frac{1}{2}, 2\right)$ does contain a factor of $\sqrt{\nu}$ and $I_\nu\left(\nu, \frac{1}{2}, 2\right)^2$, obviously a factor of ν, much in line with the more elementary lower dimensional real–complex examples studied in section 2. Further, as an exercise, we sought

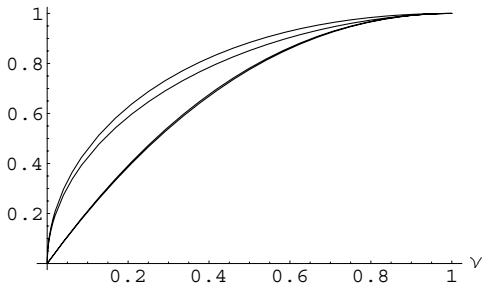

Figure 2. The most subordinate of the three curves is actually two virtually indistinguishable curves: (1) our normalized (previously obtained [9]) numerical estimate of $\mathcal{S}_{\text{complex}}(\nu)$; and (2) the (extraordinarily well-fitting) *square* of the incomplete beta function ratio $I_\nu(\nu, \frac{1}{2}, 2) = \frac{1}{2}(3-\nu)\sqrt{\nu}$. The intermediate curve is the normalized previously obtained numerical estimate of $\mathcal{S}_{\text{real}}(\nu)$ and the rather well-fitting (most dominant) curve is $I_\nu(\nu, \frac{1}{2}, 2)$.

that value of x for which the function $I_\nu\left(\nu, \frac{1}{2}, x\right)$ would when employed in our basic paradigm here, as in figure 2, *jointly* minimize the sum of a certain least-squares fit to the normalized numerical estimates of $S_{\text{real}}(\nu)$ and $S_{\text{complex}}(\nu)$. Our Mathematica program produced the answer $x = 1.88487$, being somewhat intermediate in value between $\sqrt{3} \approx 1.732$ and 2, the exact candidate values we have considered, which both fit the numerical results of [9] rather well.)

So, it would seem appropriate to revise the two central ansätze put forth in [9] to account for these interesting newly observed phenomena inherent in the results already reported in [9].

We can now exactly perform the requisite integrations (cf (17), (18)),

$$2\int_0^1 \mathcal{J}_{\text{real}}(\nu) I_\nu\left(\nu, \frac{1}{2}, 2\right) \mathrm{d}\nu = \frac{1}{151\,200} = \frac{1}{2^5 \times 3^3 \times 5^2 \times 7}, \tag{94}$$

$$2\int_0^1 \mathcal{J}_{\text{complex}}(\nu) I_\nu\left(\nu, \frac{1}{2}, 2\right)^2 \mathrm{d}\nu = \frac{71}{99\,891\,792\,000} = \frac{71}{2^7 \times 3^4 \times 5^3 \times 7^2 \times 11^2 \times 13}, \tag{95}$$

$$2\int_0^1 \mathcal{J}_{\text{quaternionic}}(\nu) I_\nu\left(\nu, \frac{1}{2}, 2\right)^4 \mathrm{d}\nu = \frac{5989}{358\,347\,086\,242\,825\,680\,000} \frac{53 \times 113}{2^7 \times 3^4 \times 5^4 \times 7^2 \times 11^2 \times 13^2 \times 17^2 \times 19^2 \times 23^2}. \tag{96}$$

The three marginal univariate Jacobian functions above are obtained by transforming the Jacobian for the Bloore parameterization—$(\Pi_{i=1}^4 \rho_{ii})^{\frac{3\beta}{2}}$, $\beta = 1, 2, 4$—to the ν variable and integrating over the two remaining independent diagonal entries of ρ.

So, assuming the validity of our modified beta function ansätze for the real and complex separability functions, all we still lack for obtaining the Hilbert–Schmidt separable volumes/probabilities of the 9-dimensional real and 15-dimensional complex qubit–qubit systems themselves are the appropriate (presumptively, exact in nature) scaling constants (on the order of 114.61 and 387.467 [9]) by which to multiply the results of (94) and (95). (We will presume—in light of the numerous analyses reported earlier—that such scaling constants are

exact in nature, being of the form $\frac{i\pi^k}{j}$, where i, j, k are natural numbers. We search over the spaces of possibilities to find choices that accord well with our previously obtained numerical results for the HS separability probabilities.)

9.1. Real two-qubit case

If we employ $\frac{20\pi^4}{17} \approx 114.599$ as the scaling constant in the real case—giving us a very good fit to the numerical estimate of $\mathcal{S}_{\text{real}}(1) \approx 114.61$—we obtain an HS separable volume of $\frac{\pi^4}{128\,520}$ and an HS separability probability of $\frac{8}{17} \approx 0.470\,588$. (Using the numerical results of [9], we were able to obtain an estimate of this probability as close as 0.469 68 by replacing the Jacobian function (15) by a sixth-order Taylor series approximation of it around $\nu = \frac{13}{16}$. Providing inferior fits to 114.61, but still of possible interest, would be choices of scaling constants $\frac{7\pi^4}{6} \approx 113.644$ and $\frac{32\pi^4}{27} \approx 115.448$. These would lead to HS real separability probabilities of $\frac{7}{15} \approx 0.466\,667$ and $\frac{64}{135} \approx 0.474\,074$—with the first of these two seeming much more consistent with the numerics of [9] than the second.)

By the (twofold) theorem of Szarek, Bengtsson and Życzkowski [20] (cf [51])—formalizing results in [18]—the HS separable volume of the generically rank-3 real qubit–qubit states would—adopting $\frac{20\pi^4}{17}$ as the appropriate scaling constant—be $\frac{\pi^4}{4760\sqrt{3}}$ and the HS separability probability, $\frac{4}{17} \approx 0.235\,294$. (The HS area–volume ratio for the nine-dimensional real two-qubit states is $18\sqrt{3} \approx 31.1769$ [1, equation (7.9)], while the analogous ratio restricted to the separable subset is one-half as large, that is, $9\sqrt{3} \approx 15.5885$, indicating the more hyperspherical-like shape of the separable subset).

9.2. Complex two-qubit case

One simple candidate for the scaling constant in the complex case is $\frac{2\pi^6}{5} \approx 384.566$. This would yield an HS separability probability of $\frac{213}{880} \approx 0.242\,045$. But considerably more attractive (certainly, in part, due to its interesting consonance with the real results just advanced, and also the presence of $256 = 2^8$ and $639 = 9 \times 71$, with the 71 in (95), thus, being canceled), it seems, is $\frac{256\pi^6}{639} \approx 385.157$ (slightly closer also to our estimate of 387.467 from [9]). This choice would yield an HS separable volume of $\frac{2\pi^6}{7023\,641\,625} \approx 2.73758 \times 10^{-7}$, and separability probability of $\frac{8}{33} \approx 0.242\,424$, *very* close to our previous numerically derived estimate of 0.242 575 (implicitly given in [18, between equations (41) and (42)] (and only slightly more than one-half of $\frac{8}{17}$). (Let us also indicate that the HS area–volume ratio for the 15-dimensional complex two-qubit states is $30\sqrt{3} \approx 51.9615$ ([equation (6.5), 1]), while the analogous ratio restricted to the separable subset is again one-half, that is $15\sqrt{3} \approx 25.9808$, the lesser value indicating the more hyperspherical-like shape of the separable subset).

In the real and complex analyses just conducted, we have tacitly assumed—as we will also do in the succeeding, remaining ones—that the appropriate scaling constants should be of the form $\frac{i\pi^k}{j}$, where, in addition to i and j being natural numbers, k is identical to the power of π occurring in the Życzkowski–Sommers/Andai formulas for the corresponding total volumes. Doing so, at least seems plausible, in light of our numerous lower dimensional analyses above.

The simplicity of two-qubit complex and real HS separability probabilities, $\frac{8}{33}$ and $\frac{8}{17}$, apparently stemming from the use of the modified beta function ansätze, now leads us to examine if we can generate somewhat parallel HS separability probabilities for the 15- and 35-dimensional real and complex qubit–*qutrit* cases.

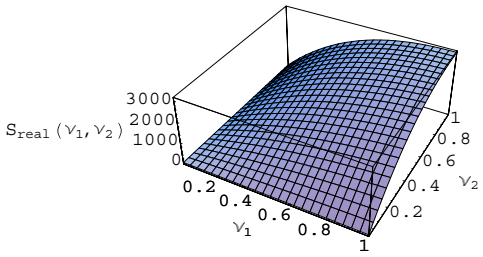

Figure 3. Interpolated estimate over the unit square of the real qubit–qutrit separability function $\mathcal{S}_{\rm real}(\nu_1, \nu_2)$, based on 785 000 randomly generated 6×6 real density matrices.

10. *Full* real and complex qubit–qutrit separability probability conjectures

10.1. Real qubit–qutrit case

In figure 3 we show an interpolated estimate (with parameter values restricted to the unit square) of the *real* qubit–qutrit separability function. (Auxiliary analyses give very strong evidence, as certainly seems plausible, that this function is *symmetric* under the interchange of ν_1 and ν_2.)

An immediate conjecture, suggested by our various earlier qubit–qutrit results (section 3 and (60)) is that this (naively, bivariate) function is actually univariate in nature, *and* satisfies the proportionality relation (cf (93))

$$\mathcal{S}_{\rm real}(\nu_1, \nu_2) = \mathcal{S}_{\rm real}(\eta) \propto I_\eta\left(\eta, \tfrac{1}{2}, 2\right) = \tfrac{1}{2}(3-\eta)\sqrt{\eta}. \tag{97}$$

Here $\eta = \nu_1\nu_2 = \frac{\rho_{11}\rho_{66}}{\rho_{33}\rho_{44}}$, being *independent* of ρ_{22} and ρ_{55} (given the definitions of ν_1 and ν_2 in equation (44) above). (If we had chosen to compute the partial transpose of ρ by transposing in place its nine 2×2 blocks, rather than its four 3×3 blocks, then presumably the same essential phenomenon would have occurred, but with different sets of indices on the ν's.) But, in fact, analyses we have conducted indicate that it is the (even simpler) univariate function satisfying the relation

$$\mathcal{S}_{\rm real}(\nu_1, \nu_2) = \mathcal{S}_{\rm real}(\eta) \propto \sqrt{\eta}, \tag{98}$$

that fits the sample estimate of the separability function displayed in figure 3 extremely well.

To substantiate this last point, in figure 4, we show a plot of a least-squares fit of the normalized function shown in figure 3 to the function η^x, which for $x = \frac{1}{2}$ is identical to (98). We see that the best fit does, in fact, suggest that $x = \frac{1}{2}$ is the appropriate choice (at least, within this one-parameter family of functions). (For the least-squares fit of (98) to our sample estimate, we obtain 0.006\,903 62, while we obtain considerably more, that is 0.018 4813, for the (inferior) fit of (97).) The product of the normalized function (98) with the corresponding Jacobian is integrable in the real qubit–qutrit case (giving the result $\frac{131\pi}{1\,110\,124\,175\,582\,822\,400} \approx 3.70723 \times 10^{-16}$).

If we adopt the ansatz (98) and employ the estimated value of the scaling constant for this function from figure 3, which is on the order of 3095.97, *and* additionally presume that the real qubit–qutrit HS separability probability (in line with our complex counterpart conjecture (immediately below) of $\frac{32}{1199}$—and qubit–qubit proposals of $\frac{8}{33}$ and $\frac{8}{17}$) is of the form $\frac{32}{k}$, where k is some natural number, then our best estimate of this probability is $\frac{32}{213} \approx 0.150\,235$, and of the scaling constant $\frac{78\,848\pi^8}{139\,515\sqrt{3}} \approx 3096.05$. (We do not have highly extensive numerical estimates (only the more limited one pursued here)—as we did in the complex qubit–qutrit

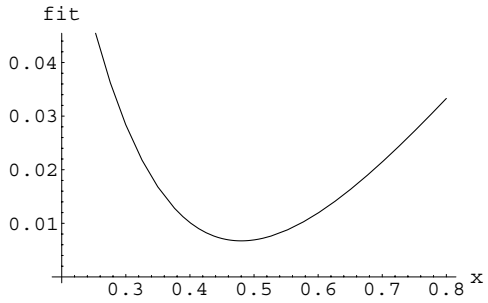

Figure 4. Least-squares fit of the normalized sample estimate of the real qubit–qutrit separability function displayed in figure 3 versus $\eta^x = (\nu_1\nu_2)^x$. The minimum of the curve is in the immediate vicinity of $x = \frac{1}{2}$, at which point the measure of goodness-of-fit is 0.006 903 62.

case [18]—against which to gauge this prediction, but our fits here are strongly supportive of these assertions. For example, our *sample* estimate of the separability probability can be expressed as $\frac{32}{213.005}$.)

10.2. Complex qubit–qutrit case

Based on our previous numerically intensive study—using 10^9 sample points—we have an (implicitly given) estimate ([18], between equations (38) and (39)) for the complex HS separability probability of 0.026 6891. A *very* well-fitting candidate for the corresponding exact probability is $\frac{32}{1199} \approx 0.026\,6889$. (The associated separable volume would, then, be $\frac{\pi^{15}}{56\,980\,588\,975\,590\,080\,071\,885\,989\,375\,000\sqrt{6}} \approx 2.05327 \times 10^{-25}$.) Aside from the striking goodness of fit, we see that the numerator of the probability is equal to $32 = 2^{n-1}$, $n = 6$, while in the qubit–qubit case, the numerator is $8 = 2^{n-1}$, $n = 4$. Also, the denominator $1199 = 109 \times 11$, while $33 = 3 \times 11$.

In line with the Dyson-indices pattern observed earlier, we investigated the possibility that the separability function in the complex qubit–qutrit case might be simply proportional to $\eta = \nu_1\nu_2$, that is, the square of its putative real counterpart, $\sqrt{\eta}$. The integral of the product of η with the associated Jacobian yields $\frac{829}{5045\,434\,342\,262\,725\,360\,252\,343\,040\,000} \approx 1.64307 \times 10^{-28}$. With our proposal above (supported by the considerable numerical evidence of [9]) that the qubit–qutrit complex HS separability probability is $\frac{32}{1199}$, the scaling constant would be $\frac{537\,472\sqrt{\frac{2}{3}}\pi^{15}}{10\,063\,956\,375} \approx 1249.65$.

Figures 5 and 6 are the *complex* qubit–qutrit counterparts of the (real qubit–qutrit) figures 3 and 4. Figure 6 might be said to weakly support the proposal that the separability function is proportional to η. (The numerics here are perhaps yet insufficient for our purposes. In addition to only so far having sampled a relatively small number of complex 6×6 density matrices, the sample points are now 30-dimensional in nature. For alacrity, we had simply used Monte Carlo methods, and not the (better behaved/'lower discrepancy') quasi-Monte Carlo (Tezuka–Faure) methods employed in our earlier studies, in particular, in [9, 18]. In light of the not very convincing nature of figure 6, it might be advisable to revert to the Tezuka–Faure scheme, although most of the unit hypercube points generated would, then, be simply discarded as not meeting the criteria a density matrix must fulfil. The most desirable/efficient sampling scheme, it seems, if it can be effectively implemented, would be the one associated

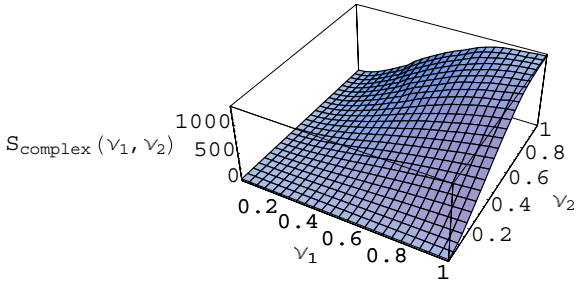

Figure 5. Interpolated estimate over the unit square of the complex qubit–qutrit separability function $S_{\text{complex}}(\nu_1, \nu_2)$, based on 880 000 randomly generated 6×6 complex density matrices.

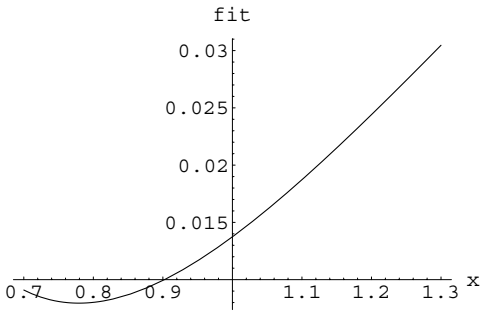

Figure 6. Least-squares fit of the normalized sample estimate of the complex qubit–qutrit separability function displayed in figure 5 versus $\eta^x = (\nu_1 \nu_2)^x$. We hypothesize that for a sufficiently large sample the minimum would lie at $x = 1$.

with correlation matrices [25, 35–37], in which *none* of the generated points would have to be discarded.

11. Concluding remarks

In a recent comprehensive review, it was stated that while quantum entanglement is 'usually fragile to environment, it is robust against conceptual and mathematical tools, the task of which is to decipher its rich structure' [52, abstract]. We have attempted to make some progress in this regard here, but considerable impediments clearly still remain to putting the chief conjectures of this paper on a fully rigorous basis (or disproving them by establishing alternative results), and in proceeding onward to higher dimensional cases. (In particular, we have not yet developed a theory to predict the scaling constants—$\frac{256\pi^6}{639}$ and $\frac{20\pi^4}{17}$ in the full complex and real two-qubit cases, and $\frac{537472\sqrt{\frac{2}{3}}\pi^{15}}{10\,063\,956\,375}$ and $\frac{78\,848\pi^8}{139\,515\sqrt{3}}$ in the full complex and real qubit–qutrit cases—for the hypothesized separability functions.) It would seem that applications and/or extensions of random matrix theory and, possibly, mathematical induction will be important—as they were in determining the total (separable *and* nonseparable) Hilbert–Schmidt volumes [1] [2, section 14.3], [5].

Let us, still, further suggest that the analytical framework and results, both theoretical and numerical, presented above may lead to the development of associated formal propositions,

much in the way that the numerically obtained (two-fold) separability-probability ratios reported in [18] led Szarek, Bengtsson and Życzkowski to establish that the set of separable (and, more generally, positive-partial-transpose) states is a convex body of constant height [20].

In [8], we have further applied the 'separability function' concept to the determination of the *Bures* (minimal monotone) metric volume of certain low-dimensional (real, complex and quaternionic) two-qubit states. Interestingly, we find that although the Dyson-index pattern is not now fully adhered too, it does come remarkably close to holding. Also, numerical research that we hope to shortly report, strongly indicates that in the full two-qubit *quaternionic* 27-dimensional *Hilbert–Schmidt* separable volume case, the Dyson-index pattern ($\beta = 1, 2, 4$) we have observed above in the two-qubit 9-dimensional real and 15-dimensional complex cases (figure 2) is strictly maintained.

Acknowledgments

I would like to express gratitude to the Kavli Institute for Theoretical Physics (KITP) for computational support in this research and to a referee for indicating that the apparent oscillatory nature of certain marginal Jacobian functions can be shown to be illusory if sufficiently high precision is used in plotting.

References

[1] Życzkowski K and Sommers H-J 2003 *J. Phys. A: Math. Gen.* **36** 10115
[2] Bengtsson I and Życzkowski K 2006 *Geometry of Quantum States* (Cambridge: Cambridge University Press)
[3] Sommers H-J and Życzkowski K 2003 *J. Phys. A: Math. Gen.* **36** 10083
[4] Slater P B 2005 *J. Geom. Phys.* **53** 74
[5] Andai A 2006 *J. Phys. A: Math. Gen.* **39** 13641
[6] Szarek S 2005 *Phys. Rev.* A **72** 032304
[7] Aubrun G and Szarek S 2006 *Phys. Rev.* A **73** 022109 (*Preprint* quant-ph/0503221)
[8] Slater P B 2007 *Preprint* 0708.4208
[9] Slater P B 2007 *Phys. Rev.* A **75** 032326
[10] Bloore F J 1976 *J. Phys. A: Math. Gen.* **9** 2059
[11] Dyson F J 1970 *Commun. Math. Phys.* **19** 235
[12] Życzkowski K, Horodecki P, Sanpera A and Lewenstein M 1998 *Phys. Rev.* A **58** 883
[13] Slater P B 2000 *Euro. Phys. J.* B **17** 471
[14] Slater P B 1999 *J. Phys. A: Math. Gen.* **32** 5261
[15] Slater P B 2000 *J. Opt. B: Quantum Semiclass. Opt.* **2** L19
[16] Slater P B 2002 *Quantum Inf. Proc.* **1** 397
[17] Slater P B 2005 *Preprint* quant-ph/0508227
[18] Slater P B 2005 *Phys. Rev.* A **71** 052319
[19] Slater P B 2006 *J. Phys. A: Math. Gen.* **39** 913
[20] Szarek S, Bengtsson I and Życzkowski K 2006 *J. Phys. A: Math. Gen.* **39** L119
[21] Gurvits L and Barnum H 2002 *Phys. Rev.* A **66** 062311
[22] Gurvits L and Barnum H 2003 *Phys. Rev.* A **68** 042312
[23] Gurvits L and Barnum H 2004 *Preprint* quant-ph/0409095
[24] Ozawa M 2000 *Phys. Lett.* A **268** 158
[25] Kurowicka D and Cooke R 2003 *Linear Algebr. Appl.* **372** 225
[26] Månsson A, Mana P G L P and Björk G 2006 *Preprint* quant-ph/0612105
[27] Månsson A, Mana P G L P and Björk G 2007 *Preprint* quant-ph/0701087
[28] Peres A 1996 *Phys. Rev. Lett.* **77** 1413
[29] Horodecki M, Horodecki P and Horodecki R 1996 *Phys. Lett.* A **223** 1
[30] Bruß D and Macchiavello C 2005 *Found. Phys.* **35** 1921
[31] Verstraete F, Audenaert K, Dehaene J and Moor B D 2001 *J. Phys. A: Math. Gen.* **34** 10327
[32] Iwai T 2007 *J. Phys. A: Math. Theor.* **40** 1361

[33] Slater P B 2006 *Preprint* quant-ph/0607209
[34] Brown C W 2001 *J. Symb. Comput.* **31** 521
[35] Kurowicka D and Cooke R M 2006 *Linear Algebr. Appl.* **418** 188
[36] Kurowicka D and Cooke R 2006 *Uncertainty Analysis with High Dimensional Dependence Modelling* (Chichester: Wiley)
[37] Joe H 2006 *J. Multivariate Anal.* **97** 2177
[38] Makhoul J 1990 *IEEE Trans. Acoust. Speech Signal Process.* **38** 506
[39] de Vicente J I 2007 Further results on entanglement detection and quantificiation from the correlation matrix criterion *Preprint* 0705.2583
[40] Gupta A K and Nadarajah S 2004 *Handbook of Beta Distribution and Its Applications* (New York: Marcel Dekker)
[41] Peres A 1979 *Phys. Rev. Lett.* **42** 683
[42] Adler S L 1995 *Quaternionic Quantum Mechanics and Quantum Fields* (New York: Oxford)
[43] Batle J, Plastino A R, Casas M and Plastino A 2006 *Preprint* quant-ph/0603060
[44] Desrosiers P and Forrester P J 2006 *Nucl. Phys.* B **743** 307–22 (*Preprint* math-ph/0509021)
[45] Verstraete F, Audenaert K and Moor B D 2001 *Phys. Rev.* A **64** 012316
[46] Augusiak R, Horodecki R and Demianowicz M 2006 *Preprint* quant-ph/0604109
[47] Eckert K, Schliemann J, Bruß D and Lewenstein M 2002 *Ann. Phys.* **299** 88
[48] Wang X, Fei S-M and Wu K 2006 *J. Phys. A: Math. Gen.* **39** L555
[49] Kimura G and Kossakowski A 2005 *Open Syst. Inf. Dyn.* **12** 207
[50] Jakóbczyk L and Siennicki M 2001 *Phys. Lett.* A **286** 383
[51] Innami N 1999 *Proc. Am. Math. Soc.* **127** 3049
[52] Horodecki R, Horodecki P, Horodecki M and Horodecki K 2007 *Preprint* quant-ph/0702225